



UNIVERSIDADE DO ALGARVE

Faculdade de Ciências e Tecnologia

**Development of a new method for the detection of
vanadium complexes bound to DNA, using Agarose
Gel Electrophoresis**

Prabal Subedi

Mestrado em Qualidade em Análises

(European Master in Quality in Analytical Laboratories)

2012



Education and Culture DG

ERASMUS MUNDUS

UNIVERSIDADE DO ALGARVE

Faculdade de Ciências e Tecnologia

**Development of a new method for the detection of
vanadium complexes bound to DNA, using Agarose
Gel Electrophoresis**

Prabal Subedi

Mestrado em Qualidade em Análises

(European Master in Quality in Analytical Laboratories)

Thesis supervised by Prof. Isabel Cavaco

2012

Acknowledgements

First of all, I would like to thank The EMQAL program and European Commission for my selection in the program. I am very thankful for my professor, Dr. Isabel Cavaco who has been very supportive during my stay here. I would also like to thank Nataliya Butenko for guiding me throughout my stay and making the lab environment very enjoyable. I am thankful to Dr. Jorge Martins and Miguel Manuel for helping me use the equipments. My sincere gratitude goes to the International Mobility office for helping me with finding accommodation and taking care of my other bureaucratic problems. My thanks also go to Dr. Helio and his team for helping me with the instruments that I needed to use during my stay. I would like to express my gratitude for Cláudia Albaça and Débora Mendes for the translation of my abstract in Portuguese.

Table of Contents

LIST OF FIGURES.....	1
LIST OF TABLES.....	2
LIST OF ABBREVIATIONS AND TERMINOLOGY	3
RESUMO.....	4
ABSTRACT	6
1. INTRODUCTION	8
1.1. DNA-a brief overview	8
1.2. Cleavage of DNA.....	9
1.2.1. Hydrolytic cleavage.....	9
1.2.2. Oxidative Cleavage.....	11
1.3. Inorganic Nucleases	12
1.3.1. Vanadium Nucleases	13
1.3.2. Ruthenium Nucleases	14
1.4. Analytical methods for the study of inorganic nucleases	16
1.5. Aim of the project	19
1.6. Chemistry of the method.....	20
1.6.1. Fenton Reaction.....	20
1.6.2. TPA(terephthalic acid) Hydroxylation	21
1.7. Techniques used.....	23
1.7.1. Agarose Gel Electrophoresis (AGE)	23
1.7.2. Absorption Spectrometry.....	25
1.7.3. Fluorescence Spectroscopy.....	26
1.8. Method validation parameters	28
1.8.1. LOD (limit of detection).....	28
1.8.2. Sensitivity	28
1.8.3. Precision	29

1.8.4.	Estimation of errors	29
2.	EXPERIMENTAL SECTION	30
2.1.	Instruments.....	30
2.2.	Preparation of solutions	30
2.2.1.	Phosphate buffer:.....	30
2.2.2.	TPA(Terephthalic acid) solution	30
2.2.3.	Concentrated TBE solution	30
2.2.4.	Water	30
2.2.5.	Vanadium complexes solution	31
2.2.6.	Hydrogen Peroxide	31
2.3.	Spectrofluorimetric measurements	31
2.3.1.	Preparation of solutions	31
2.3.2.	Fluorescence measurement.....	32
2.4.	Agarose gel preparation.	33
2.4.1.	Agarose Gel Electrophoresis	33
2.4.2.	Agarose gels for testing the Fenton-like reaction coupling with TPA hydroxylation.....	34
2.4.3.	Agarose gels in cuvette.....	35
3.	RESULTS AND DISCUSSION.....	36
3.1.	Agarose gel electrophoresis	36
3.2.	Preliminary tests in agarose gel.	36
3.3.	TPA-hydroxylation coupled with Fenton-like reactions	37
3.3.1.	Method development in aqueous solutions.	37
3.3.2.	With D-galactose	43
3.4.	Fluorescence in agarose gels.....	48
3.4.1.	Boiling and dissolving agarose only with TPA.....	48
3.4.2.	Boiling and dissolving agarose with TPA,VO(acac) ₂ and H ₂ O ₂	48

3.5.	Stability of Hydrogen Peroxide	50
3.6.	Choice of excitation wavelength.....	50
4.	CONCLUSIONS.....	51
4.1.	Aqueous system	51
4.2.	Aqueous system containing galactose	51
4.3.	Agarose gels.....	51
4.4.	Overall	51
5.	BIBLIOGRAPHY.....	52
5.1.	References.....	52

List of Figures.

Figure 1. A monomer of the DNA molecule.	8
Figure 2. Three forms of plasmid DNA- supercoiled (Form I), nicked (Form II) circular and linear(Form III) ³	9
Figure 3. Mechanism of hydrolytic cleavage ³	10
Figure 4. Different proposed activation modes for hydrolysis of phosphodiester bonds: (a) lewis acid activation, (b) nucleophile activation, (c) leaving group activation, (d) metal coordinated hydroxides and (e) metal coordinated water molecule. (M denotes metal complex)	11
Figure 5. Mechanism of oxidative cleavage.	12
Figure 6. Vanadium compounds BMOV, BEOV and VO(acac) ₂	14
Figure 7. Ruthenium complexes KP1019 and NAMI-A.	15
Figure 8. AGE(3h, 110 V) of DNA samples incubated with VO(acac) ₂ and VO(Cl _o r) for 1h at 37 ⁰ C.....	18
Figure 9. TPA hydroxylation.	22
Figure 10. Fenton-like reaction coupled with TPA-hydroxylation.	23
Figure 11. Instrumental set-up for AGE	24
Figure 12. Light passing through a cuvette	25
Figure 13. Schematic diagram of a spectrophotometer ⁵⁷	26
Figure 14. Jablonski Diagram illustrating the absorption and the emission processes. .	27
Figure 15. Schematic diagram of a spectrofluorometer ⁶⁰	28
Figure 16. Procedure of spectrofluorimetric measurement	32
Figure 17. The position of samples of vanadium in 1% agarose gel containing 200 μM TPA.....	34
Figure 18. Gel imaging of experiment from Figure 17 before addition of H ₂ O ₂ (left) and after addition of H ₂ O ₂ (right). [Excitation at 302 nm and filter at (595 ± 40) nm] .	36
Figure 19. Time evolution of maximum intensity (410 nm) of 2-OH-TPA generated from different concentrations of VO(SO ₄) over time. H ₂ O _{2conc} = (~9M)	37
Figure 20. Time evolution of maximum intensity (410 nm) of 2-OH-TPA generated from different concentrations of VO(acac) ₂ over time. H ₂ O _{2conc} = (~9M).....	38

Figure 21. Fluorescence spectra measurements for 80 μ M VO(acac) ₂ over time. H ₂ O _{2conc} = ~9M.....	39
Figure 22. Figure showing the different positions in the benzene ring where hydroxylation can take place when large excess of .OH radicals are present.	39
Figure 23. Time evolution of maximum intensity (428 nm) of 2-OH-TPA generated from concentrations of VO(acac) ₄ over time. H ₂ O _{2conc} = 1,8M	40
Figure 24. Individual fluorescence spectrum measurements.....	41
Figure 25. Maximum intensity (428nm) of 2-OH-TPA with different concentrations of VO(acac) ₂ over time. H ₂ O _{2conc} = 1,8 mM.....	42
Figure 26. Individual fluorescence spectrum measurements for different concentrations of VO(acac) ₂ in presence of 0,050% D-galactose. H ₂ O _{2 conc} =1,8 mM.....	44
Figure 27. Maximum intensity (428nm) of 2-OH-TPA generated from different concentrations of VO(acac) ₂ over time. H ₂ O _{2conc} = 1,8 mM, galactose= 0,050%.....	45
Figure 28. Maximum intensity (428nm) of 2-OH-TPA generated from different concentrations of VO(acac) ₂ over time. H ₂ O _{2conc} = 1,9 mM, galactose= 0,50%.....	46
Figure 29. Maximum intensity (428nm) of 2-OH-TPA generated from different concentrations of VOSO ₄ over time. H ₂ O _{2conc} = 1,8 mM, galactose= 0,50%.	46
Figure 30. Maximum intensity (428nm) of 2-OH-TPA generated from different concentrations of VO(acac) ₂ over time. H ₂ O _{2conc} = 1,9 mM, galactose= 0,50%.....	47
Figure 31. Fluorescence spectra measurement of 1% agarose gels containing 200 μ M TPA and 1,8 mM H ₂ O ₂	49
Figure 32. Absorbance of hydrogen peroxide over time.	50

List of tables

Table 1. Parameters to study the sensitivity at different time intervals for TPA hydroxylation coupled to Fenton-like reactions. The errors are presented with 95% confidence intervals.....	43
Table 2. A comparison (at 5 min) between the sensitivities when different wt% of galactose was used. The values are presented with 95% confidence intervals.	47

List of abbreviations and terminology

Abbreviations	Meaning
μ_i°	absolute electrophoretic mobility
AFM	atomic force microscopy
AGE	agarose gel electrophoresis.
b	y-intercept
BEOV	bis(ethylmaltolato)oxovanadium(IV)
BMOV	bis(maltolato)oxovanadium(IV)
CE	capillary electrophoresis
DNA	deoxyribonucleic acid
EtBr	ethidium bromide
F_d	frictional force
F_e	electrical force
k	constant
LOD	limit of detection
m	slope
PAGE	polyacrylamide gel electrophoresis
ROS	reactive oxygen species
Salen	salicylaldehyde and ethylenediamine
sd	standard deviation
TPA	terephthalic acid
v_i°	velocity of particle
η	fluid viscosity

Resumo

Existem apenas alguns métodos disponíveis para o estudo da ligação de metais ao ADN. Estes são baseados em técnicas espectroscópicas, que podem apenas ser utilizadas quando determinados cromóforos quer da molécula de ADN ou dos complexos metálicos estão directamente envolvidos na ligação de metais ao ADN.

O objectivo deste projecto foi desenvolver um novo método que pode ser utilizado para detectar a ligação de um metal de transição ao ADN, utilizando Electroforese em gel de agarose (EGA). O método tem sido estudado para complexos de vanádio, mas pode ser adaptado para quaisquer metais de transição susceptíveis de sofrer reacções de tipo Fenton. O novo método envolve a adição ao gel de agarose de ácido tereftálico (TPA), um indicador bem conhecido para os radicais hidroxilo. Embebendo o gel desenvolvido em peróxido de hidrogénio, a presença de vanádio será revelada por uma reacção do tipo Fenton que irá gerar radicais hidroxilo e irá hidroxilar TPA em 2-hidroxi-TPA, uma molécula altamente fluorescente. Bandas electroforéticas contendo vanádio podem então ser fotografadas e analisadas utilizando um sistema de imagem.

A metodologia envolveu quatro passos:

1. Um estudo preliminar do sistema utilizando a EGA.
2. O desenvolvimento do método para a quantificação dos complexos de vanádio baseado no mesmo sistema de reacção utilizando amostras aquosas.
3. Desenvolvimento do método em soluções aquosas com uma matriz semelhante à de agarose.
4. Aplicação em géis de agarose.

Os resultados preliminares foram mal sucedidos para detectar a presença de vanádio em géis de agarose. Concluiu-se que para ser usado um sistema de imagem, o método requer a utilização de um filtro (464 ± 40) nm. Foram efectuados mais testes utilizando um espectrofluorímetro.

Quando se utilizou um concentrado peroxide ($\sim 9M$), a intensidade máxima de fluorescência de 2-OH-TPA formado diminuiu ao longo do tempo. Com um peróxido

menos concentrado (1,8 mM) foi obtida uma boa sensibilidade. O LOD (limite de detecção) determinado para o vanádio foi de 4,1 μM .

O sistema foi depois testado num sistema aquoso com galactose. O sistema tem uma boa gama de trabalho, até 300 μM na presença de 0,50% de galactose. A sensibilidade diminuiu significativamente na presença de galactose. O LOD determinado para o vanádio foi de 5,4 μM .

O sistema foi finalmente testado em géis de agarose. Houve alguma dificuldade em assegurar a homogeneidade da preparação, necessária para um estudo espectrofluorimétrico. Num gel onde a homogeneidade foi conseguida, foi observada uma banda de emissão muito fraca na região do espectro onde o complexo 2-hidroxi-TPA emite. A sensibilidade obtida nesta preparação foi muito baixa.

Não foi possível completar os testes em EGA devido à falta de tempo disponível para este trabalho. No entanto, os resultados em solução aquosa mostram que o método é viável e pode proporcionar uma boa sensibilidade quando aplicado em matrizes EGA, desde que o método para a preparação de gel seja optimizado.

Palavras-chave: nucleases de vanádio, eletroforese em gel de agarose, espectrofluorimetria, desenvolvimento do método, interacção metal-ADN.

Abstract

There are few methods available for the study of the binding of metals to DNA. These are based in spectroscopic techniques which can only be used when certain chromophores, either from the DNA molecule or from the metal complexes, are directly involved into the binding of metals to DNA.

The objective of this project has been to develop a new method that can be used to detect the binding of a transition metal to DNA using Agarose Gel Electrophoresis. The method has been studied for vanadium complexes, but can be adapted to any transition metals that can undergo Fenton-like reactions. The new method involves the addition to the agarose gel of terephthalic acid (TPA), a well-know indicator for hydroxyl radicals. By soaking a developed gel in hydrogen peroxide, the presence of vanadium will be revealed by a Fenton-like reaction that will generate hydroxyl radicals and will hydroxylate TPA into 2-hydroxy-TPA, a strongly fluorescent molecule. Electrophoretic bands containing vanadium can then be photographed and analysed using an imaging system.

The methodology followed four steps:

1. A preliminary study of the system using AGE.
2. The development of the method for the quantification of vanadium complexes based on the same reaction system using aqueous samples.
3. Development of the method in aqueous solutions with a matrix as similar as possible to agarose.
4. Application in agarose gels.

Preliminary results were unsuccessful in detecting the presence of vanadium in agarose gels. It was concluded that to be used in an imaging system the method would require the use of a (464 ± 40) nm filter. Further testing was done using a spectrofluorimeter.

When concentrated peroxide (~ 9 M) was used, the maximum fluorescence intensity of 2-OH-TPA formed decreased over time. With a less concentrated peroxide (1,8 mM), a good sensitivity was obtained. The LOD (limit of detection) for vanadium was determined to be 4,1 μ M.

The system was then tested in aqueous system with galactose. The system has a good working range for up to 300 μM when 0,50% galactose was present. The sensitivity decreased significantly in the presence of galactose. The LOD for vanadium was established to be 5,4 μM .

The system was finally tested in agarose gels. There were major issues in assuring the homogeneity of the preparation, necessary for a spectrofluorimetric study. In one gel where homogeneity was achieved, a very weak emission band was observed in the spectral region where 2-hydroxy-TPA emits. The sensitivity obtained in this preparation is very low.

It was not possible to complete the tests in AGE because of time impediments for this work. Nevertheless, the results in aqueous solution show that the method is viable and should provide a good sensitivity when applied in AGE matrices, provided the method for the preparation of gel is optimized.

Key Words: vanadium nucleases, agarose gel electrophoresis, spectrofluorometry, method development, metal-DNA interaction.

1. INTRODUCTION

1.1. DNA-a brief overview

DNA (Deoxyribonucleic acid) (**Figure 1**) is a polymer of nucleic acid containing the genetic information for living organisms. It has a deoxyribose sugar and a nitrogen base (purine: adenine and guanine; pyrimidine: thymine and cytosine). The individual units are joined together by strong phosphodiester bonds from the 3' of one unit to 5' of another unit. In DNA, the strands run antiparallel to each other and hydrogen bonding between the nitrogen bases provides the stability between the two strands. The phosphodiester bonds in the DNA have a half life ($t_{1/2}$) of 130,000 years at neutral solution and at room temperature¹. Any possible nucleophile is repelled by the negative charges in the sugar phosphate backbone² and therefore the DNA is very stable molecule.

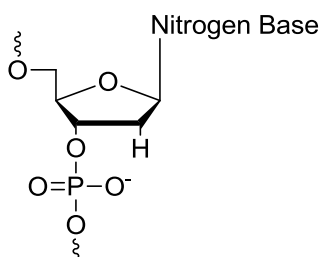


Figure 1. A monomer of the DNA molecule.

DNA is a stable molecule and it creates a serious obstacle in DNA manipulation, namely, expression and duplication, repair of damaged DNA and elimination of foreign DNA. To overcome this obstacle, nature has come up with hydrolytic enzymes, topoisomerases and nucleases that catalyze the scission of DNA³. These enzymes contain certain metal ions such as Ca(II)³ Mg(II)⁴ and Zn(II)⁵ as cofactors and they play a very important part in the catalytic action.

DNA can be further classified into genomic DNA (present in all living organisms) and plasmid DNA (found mostly in bacteria, or mitochondria/chloroplasts in higher organisms). In most biological systems, plasmid DNA is present as supercoiled form (Form I)(**Figure 2**). This form is important for gene expression, DNA replication and

recombination. If there is a nicking in one of the strands, it will result in loss of supercoils and the DNA will be in nicked form (Form II), or also called open circular form. If there is a nicking in both the strands at the (nearly) same points, the DNA will arrange itself into a linear form (Form III)⁶.

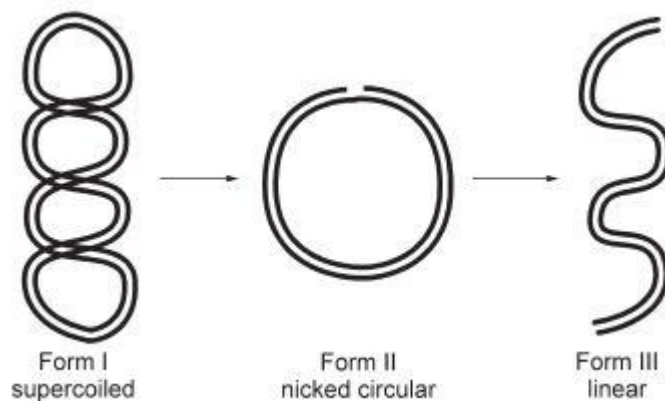


Figure 2. Three forms of plasmid DNA- supercoiled (Form I), nicked (Form II) circular and linear(Form III)³

1.2. Cleavage of DNA

Since the nature uses many metallic ions for the interactions with biological molecules⁷, the humankind has attempted to reproduce those biological activities with artificial compounds. The results include the synthesis of many inorganic complexes that have shown promising results in the medicinal field. The cleavage of DNA is no exception. DNA cleavage can be achieved by inorganic complexes and these complexes are called *inorganic nucleases*⁸. The cleavage in DNA takes place mainly by two possible mechanisms- hydrolytic and oxidative cleavage.

1.2.1. Hydrolytic cleavage

An interest in hydrolytic cleavage comes from the fact that the mechanistic information obtained from such studies would help better understanding of hydrolytic enzymes. Also, the hydrolytic agents could be used to detoxify pesticides and chemical agents, as the pesticides and chemical agents often contain phosphate-ester like structures³. Since reported by J.K. Barton⁹ in 1987 the first artificial hydrolytic agent, much interest is present in the scientific world for these complexes. Hydrolysis by natural nucleases is assumed to proceed via a 5 coordinated transition state¹⁰ and furthermore cleavage on P-O3' produces the breakdown products.

Figure 3 shows the mechanism for hydrolytic cleavage.

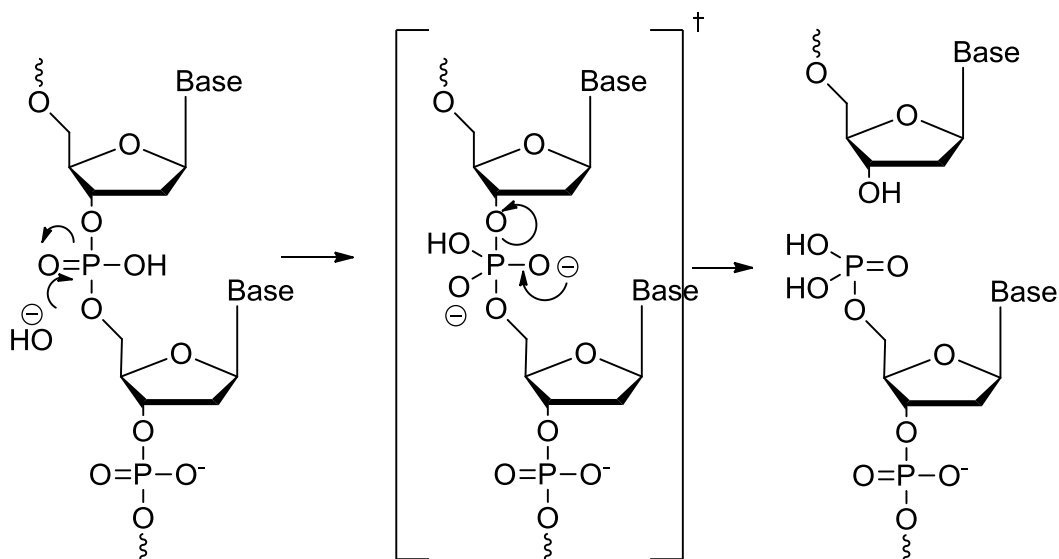


Figure 3. Mechanism of hydrolytic cleavage³

Metal ions and their complexes help facilitate faster reactions. There are various activation modes by which the metal ions could facilitate the hydrolysis of phosphate diesters. The different proposed modes (**Figure 4**) are lewis acid activation, nucleophile activation, leaving group activation, metal coordinated hydroxides and metal coordinated water molecule^{2, 3,11}. When metals with redox chemistry are employed, another form of cleavage-*oxidative cleavage* could also take place³.

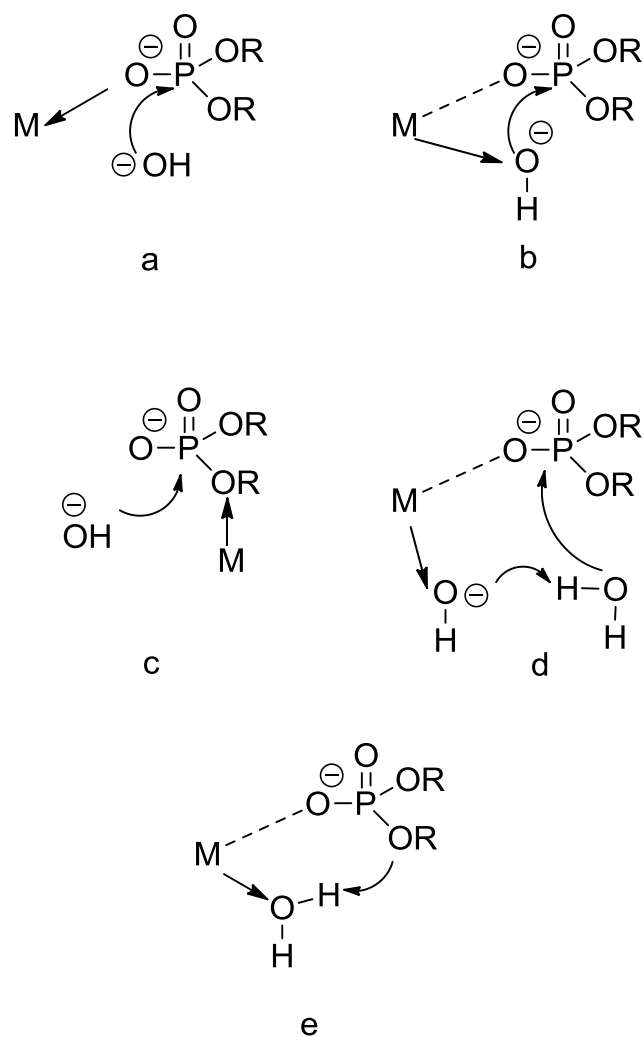


Figure 4. Different proposed activation modes for hydrolysis of phosphodiester bonds: (a) lewis acid activation, (b) nucleophile activation, (c) leaving group activation, (d) metal coordinated hydroxides and (e) metal coordinated water molecule. (M denotes metal complex)

1.2.2. Oxidative Cleavage

Cu(II) and Fe(III) have been known to cleave DNA in an oxidative way. Also reported are transitional metal complexes in the presence of oxidants/reductants or without external agents¹². The cleavage can occur either in the nitrogenous base or in the ribose sugar. The agents responsible are called reactive oxygen species (ROS) which include superoxide and hydroxyl radicals, single oxygen and high valence metal oxo species¹³. Since, there are 4 nitrogenous bases and different ROS and the fact that the oxidation could occur either in the base or in the sugar ring, various mechanisms of oxidations are possible. One such oxidative mechanism by Fe^{II}Bleomycin^{14,15} is given in **Figure 5**.

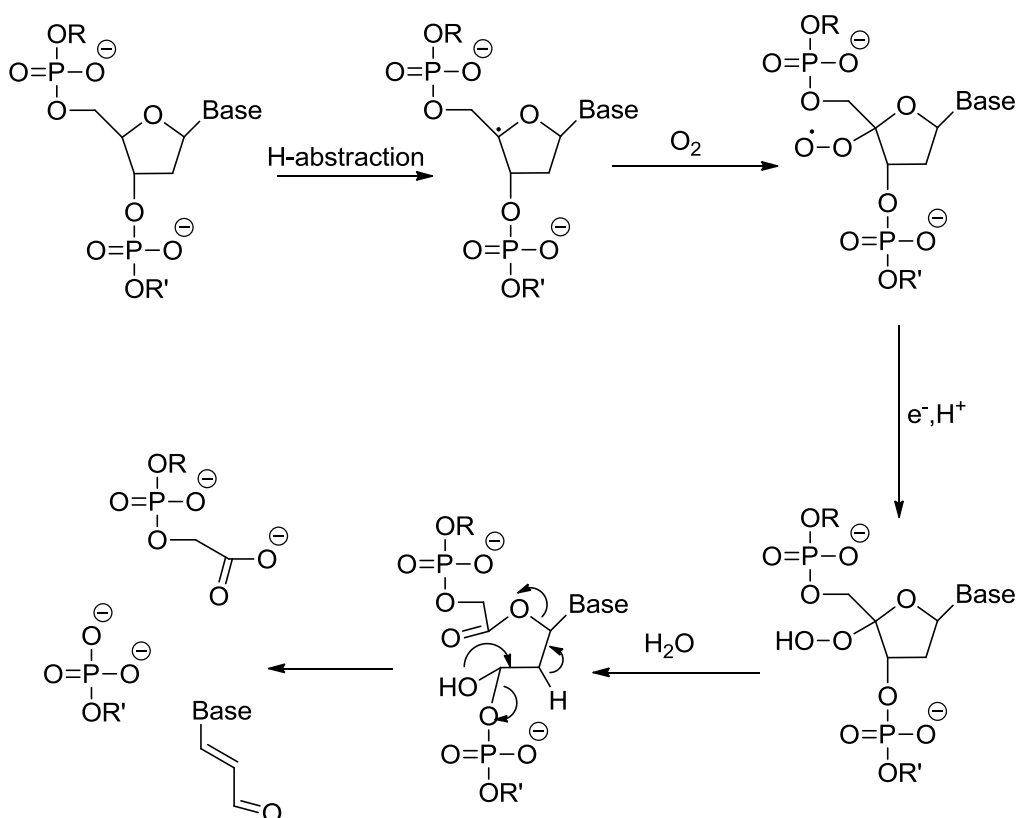


Figure 5. Mechanism of oxidative cleavage.

1.3. Inorganic Nucleases

Although the field of medicinal chemistry has been largely dominated by organic chemistry, the advancement in research of metal based drugs has grown over the past years⁷. Platinum compounds were one of the first metal based complexes to be used as antitumor agents¹⁶. Numerous others inorganic complexes have been discovered to have medical applications.

Among the applications, gene manipulation has been a hot topic. Certain metal complexes have shown promising results as DNA probes¹⁷, DNA targeting antitumor agents¹⁸ and in nucleic acid mapping¹⁹. En route towards gene manipulation, synthetic nucleases have attracted much attention with regards to their applications. The nucleases will not only be able to reveal the restriction enzyme mechanism but also as

conformational probes for DNA structure, antibiotic and chemotherapeutic drugs. In fact, they might even be more efficient cleavers of DNA than natural enzymes²⁰. Among the metals that mediate DNA oxidation, transitional metal complexes of Fe, Cu, Ni, Pt, Ru, Rh, V, Cr, Co, Mn and Os have been reported¹². Some of them are explained below.

1.3.1. Vanadium Nucleases

Although vanadium exists in III, IV or V oxidation states in aqueous media²¹, the oxidation state of vanadium in the biological system is debatable. While some argue that there is interconversion of V(IV) and V(V) species in the blood²², others state that regardless of the species injected, the fate of vanadium in the biological system ends up with V(IV)²³. Also, the exact mechanism of how vanadium cleaves DNA is unknown.

Vanadium complexes, already known for their insulin mimetic activity²⁴, were first reported in 1996 for their nuclease activity²⁵. The complexes that have proven to reduce the plasma glucose levels in streptozotocin-induced diabetic rats are bis(maltolato)oxovanadium(IV) (BMOV) and bis(ethylmaltolato)oxovanadium (IV) (BEOV)²⁶ (**Figure 6**). BEOV has passed clinical trials phase I and phase II⁷. Other orally active compounds that have been studied as treatment for diabetes contain the oxidation state vanadium (IV)²⁴.

Vanadium(IV) compounds of salen(salicylaldehyde and ethylenediamine) derivatives cleaved DNA at guanine residues in presence of oxone. Proposed mechanisms included the formation of oxidation of V(IV) to V(V) and the production of $\text{SO}_4^{\cdot-}$ and $\text{SO}_5^{\cdot-}$ radicals²⁷. Similarly, some oxovanadium (IV) schiff base complexes have demonstrated nuclease activity in UV-A light of 365 nm via the $^1\text{O}_2$ pathway and via OH^{\cdot} pathway in presence of near-IR light(752.5-799.3 nm IR optics)²⁸.

Although most studies are done with vanadium(IV) complexes, there are a handful of reports on vanadium(III) and vanadium(V) nucleases. Bis(peroxo)vanadium(V) phenanthroline promotes a single strand DNA cleavage. During photooxidation of peroxo ligands, OH^{\cdot} are produced and this leads to the strand cleavage²⁹. Vanadium(III) phenanthroline and bipyridine dimers were found to have very strong interaction with DNA that ultimately led to the degradation of DNA³⁰.

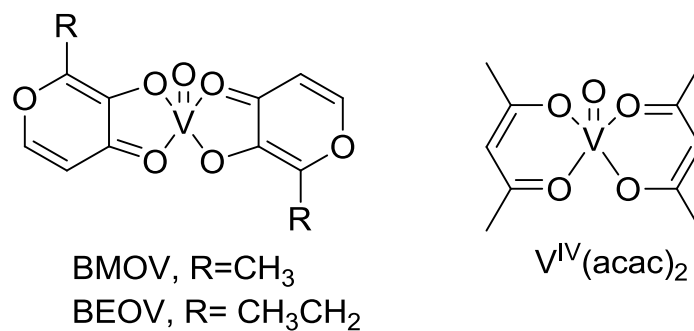


Figure 6. Vanadium compounds BMOV, BEOV and VO(acac)₂.

Another compound, VO^{IV}(acac)₂ (**Figure 6**) that has been known for insulin enhancing activity²⁴, has also shown promising results in DNA cleavage. VO(acac)₂, above 1 μm has been reported as a very efficient cleavage agent. Moreover, it requires no activating agents such as air or irradiation. However, the use of buffer plays an important role for this compound⁸.

1.3.2. Ruthenium Nucleases

Ruthenium complexes have been a part of research interest over the past few years. Ruthenium complexes are one of the very few metal complexes to be studied as anti-cancer drugs. Two important complexes are KP109 and NAMI-A (**Figure 7**). NAMI-A possesses high and selective anti-metastatic activity and has passed Phase I clinical trials (the first ruthenium antitumor complex to enter the trials)³¹ but has failed the screening for antitumor drugs³². KP1019 demonstrates antineoplastic activity against a wide number of tumors³³.

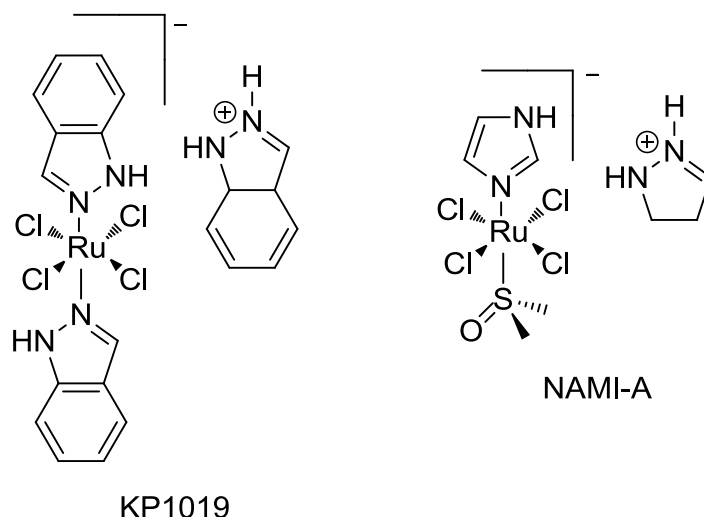


Figure 7. Ruthenium complexes KP1019 and NAMI-A.

The targets of Ruthenium based complexes are still arguable⁷. NAMI-A and KP1019 can irreversibly coordinate with DNA^{32,34}. Nevertheless, Plasma proteins and glutathione are believed to be more essential than DNA for the antitumor activities for NAMI-A and KP1019³². Ru-arene complexes can interact with DNA via direct coordination to the bases, intercalation and stereospecific H-bonding³⁵. Ruthenium(III) complexes with ligands phenanthroline, bipyridine, dipyridoquinoxaline and dipyridophenazine were found to bind to DNA in a non-covalent way before cleaving them³⁶.

Similarly, ruthenium(II) polypyridyl complex was found to hydrolytically cleave DNA in a enzyme-like manner³⁷. A Ru(II) dimer was found to cleave DNA under anerobic conditions after undergoing an in situ reduction. When exposed to air, together with large amount of reducing agents, the cleavage activity was diminished. This could provide a means of selective cleavage activity for cells with low oxygen content³⁸. Ruthenium(II) nitrofurylesemicarbazone complexes were revealed to affect the DNA conformation and also cleave it via oxidative mechanism. It was believed that the compound interacts with the minor groove in DNA³⁹.

However, ruthenium nucleases are relatively “new” in the field of inorganic nucleases and an in depth study is required for these complexes.

1.4. Analytical methods for the study of inorganic nucleases

Inorganic nucleases can be even more effective than natural nucleases and also cheaper. Therefore, there is a bright future in the field of inorganic complexes as DNA cleavers. To study the interactions of metal complexes many analytical methods have been used. Spectrometric techniques such as UV/VIS absorption spectroscopy, CD (circular dichroism) fluorescence spectroscopy, electro-analytical techniques such as voltametric techniques, imaging techniques such as AFM(atomic force microscopy) are widely used to study the interaction of the metal/metal complexes with DNA.

Separation techniques such as capillary electrophoresis (CE) and gel electrophoresis – agarose gel electrophoresis (AGE) and polyacrylamide gel electrophoresis (PAGE) are used for studies of DNA. Electrophoresis is a technique where the molecules are separated by their charge and their size. The charged molecules are placed in an electric field. The particles are accelerated by the electrical force, F_e :

$$F_e = Z_i \cdot e \cdot E \quad \text{Eq. 1}$$

Where,

- Z_i = charge of the particle/component I
 e = elementary charge ($1,602 \times 10^{-19}$ C)
 E = electric field strength ($\text{V}\cdot\text{cm}^{-1}$)

However, when the particles are accelerated, there is a frictional force (F_d) present which slows the movement. Considering that the moving particles are spherical, F_d is given as

$$F_d = k \cdot \eta \cdot v_i^o \quad \text{Eq. 2}$$

Where,

- η = fluid viscosity ($\text{P}_a \cdot \text{s}$)
 k = constant (cm)
 v_i^o = velocity of particle ($\text{cm} \cdot \text{s}^{-1}$)

For a spherical particle, according to the Stokes' law, k is given as,

$$k = 6 \pi r_i \quad \text{Eq. 3}$$

Where,

r_i = radius of the component/sphere

So, when an electrical field is established, the electrical force is balanced by the frictional force, and therefore, the particle moves at a terminal velocity v_i^o

$$F_d = F_e \quad \text{Eq. 4}$$

$$6 \pi r_i \eta v_i^o = Z_i \cdot e \cdot E \quad \text{Eq. 5}$$

$$v_i^o = \frac{Z_i \cdot e}{6 \pi r_i \eta} E \quad \text{Eq. 6}$$

The terminal velocity, v_i^o , is proportional to the electrical field E and the proportionality constant is called the absolute electrophoretic mobility, μ_i^o ($\text{cm}^2\text{V}^{-1}\text{s}^{-1}$) or

$$\mu_i^o = \frac{v_i^o}{E} = \frac{Z_i \cdot e}{6 \pi r_i \eta} \quad \text{Eq. 7}$$

For large molecules such as DNA, the mobility also depends upon on the shape of the molecule.

There are different kind of electrophoresis types including but not limited to capillary electrophoresis, isotachopheresis and gel electrophoresis. Gel electrophoresis is relatively easy to carry out and is often a widely used technique for the study of DNA and its interaction with metal complexes.

At neutral pH, the DNA is negatively charged. Therefore, when an electric field is applied, the molecules migrate towards the positive pole. The migration occurs through the gel matrix. Gel matrices consist of pores and these pores sieve the DNA molecules according to its volume. The smaller molecules pass easily as they have a lesser effective volume than the bigger ones. The visualization of DNA is done by staining by fluorescent dyes such as ethidium bromide (EtBr). EtBr has planar rings and it intercalates between the stacked bases in the nucleotide. When exposed to ultraviolet

light, this intercalation increases intensely the fluorescence of EtBr and thus the DNA can be visualized.

The gel matrices that are used are polyacrylamide and agarose. Agarose is a linear polymer of agarobiose. Agarobiose is a disaccharide made up of D-galactose and 3,6-anhydro-L-galactopyranose⁴⁰. Polyacrylamide is a cross linked polymer of acrylamide. Polyacrylamide has smaller pores and a high resolving capacity but only over a narrow size range (eg. a few base pairs). However, during cleavage of DNA, the new fragments could differ to each other by hundreds of base pairs and therefore agarose gels provide a better resolution. A nicked or a circular DNA moves more slowly than a supercoiled DNA which is compact and has a small effective volume, thus helping them to migrate more rapidly during electrophoresis⁴¹.

One such electrophoresis (AGE) of plasmid DNA after incubation with vanadium complexes (details in the experimental section) is shown in **Figure 8**.

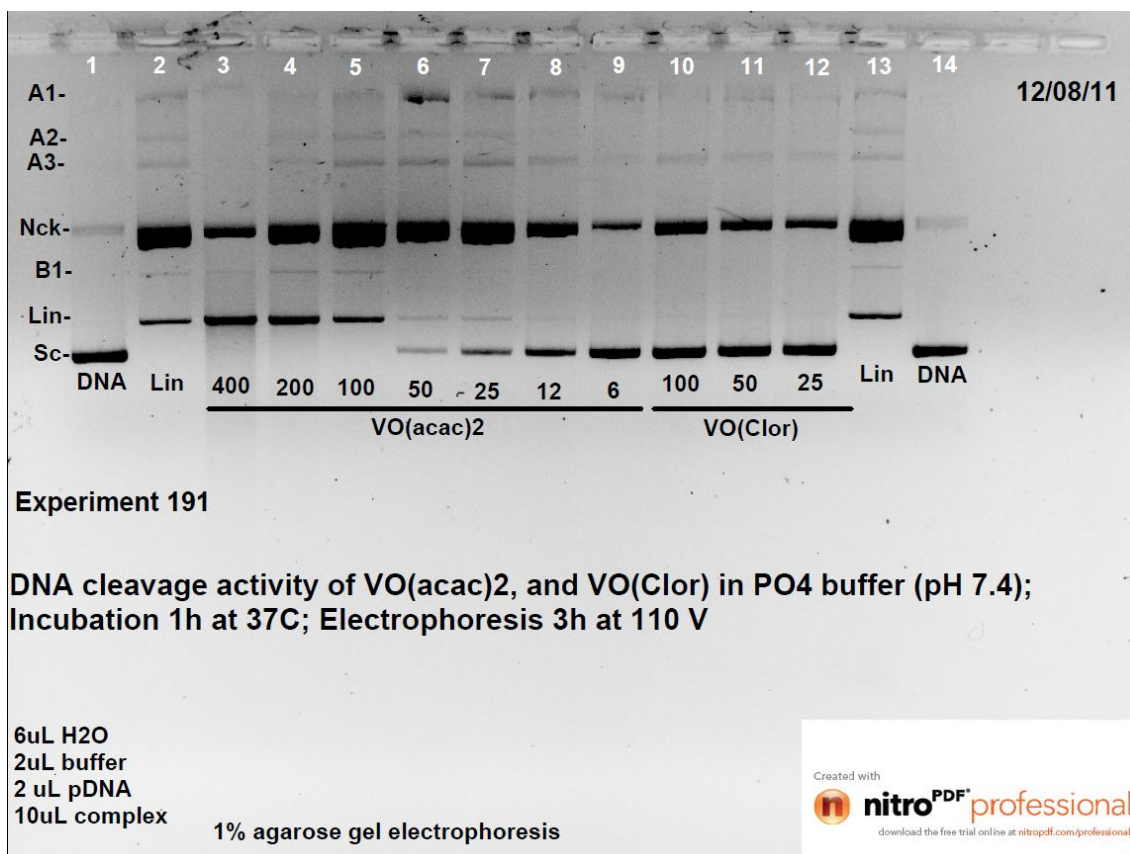


Figure 8. AGE(3h, 110 V) of DNA samples incubated with VO(acac)₂ and VO(ClO₄)₃ for 1h at 37⁰C

It can be observed that there are mainly 3 main bands- of supercoiled (Sc), linear (Lin) and nicked (Nck). The extremes (1 and 14) wells contained non-incubated plasmid DNA and wells (2 and 13) contained linearised DNA.

1.5. Aim of the project

When performing AGE of plasmid DNA digested with vanadium nucleases, a number of unexplained weak bands are often observed. These can be viewed in **Figure 8**: band A1, A2, A3 and B1. These bands have been named ‘Phantom bands’ and will be referred as same in the rest of the manuscript. Some characteristics of these bands are-

- a. These bands were present in samples that contained vanadium complexes but not in the native DNA sample (1 and 14 wells). This indicates the effect is provided by incubation with the vanadium complexes.
- b. The bands increased in intensity with the increase in concentration of the vanadium complexes.
- c. These bands always appear at the same place in the gel.

There have been a few possible explanations thought of for these bands. The DNA molecules in bands A1, A2 and A3 have a lower electrophoretic mobility than the 3 plasmid DNA bands (supercoiled, nicked and linear). The factors that the electrophoretic mobility depends on are size, charge and the shape of the molecules. Since the viscosity of the medium is same for all the bands, the size and charge of the molecules in phantom bands are a question.

Charge of the molecules: When the electrophoresis is performed at neutral pH, the DNA is believed to be negatively charged. However, during incubation with vanadium complexes, there could have been some binding of the metal complex with the nucleic acid and eventually neutralizing some of the charges in the DNA backbone. This would lower the charge in the molecule and thus finally lowering the overall charge of the molecule resulting in a smaller effective mobility.

Size and shape of the molecules: During the incubation of DNA samples with the vanadium complexes, the complexes could have created an environment where the strands could have agglomerated and thus the size of the molecule increased thus lowering the mobility in the gels. Or, perhaps, the incubation could have changed the

shape of the DNA molecules from the globular shape(as one might expect) and thus the migration in the gels is distorted.

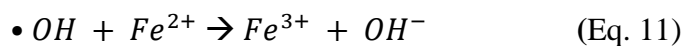
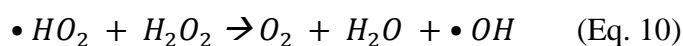
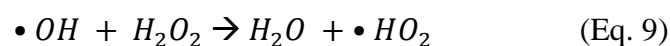
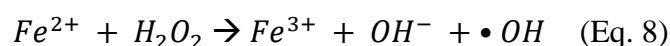
Thus, the project was to develop a method to detect and quantify vanadium bound to the DNA molecules, using AGE. This method could also be extended for detection and quantification of other metals that take part in the Fenton-like reaction. The steps of the project are-

- a. First to develop a method in quantifying the metal using aqueous solutions, then optimize the time of reactions and the concentration of reagents to obtain the best possible sensitivity at a reasonable analysis time.
- b. To be able to transfer the method to real matrix(agarose gel after the electrophoresis)
- c. Detection of the band by means of UV/VIS imaging.

1.6. Chemistry of the method

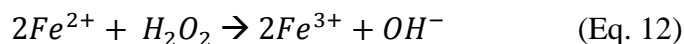
1.6.1. Fenton Reaction

According to the IUPAC definition, Fenton reaction is the iron-salt dependent decomposition of dihydrogen peroxide, generating the highly reactive hydroxyl radical, possibly via an oxoiron(IV) intermediate. Addition of a reducing agent, such as ascorbate, leads to a cycle which increases the damage to biological molecules. (-It was first discovered by Henry Fenton⁴². Haber and Weiss later discovered the Fenton reaction was both a radical and a chain reaction. They also described following set of equations of the reaction⁴³ -



The later revised form of the reaction by Barb⁴⁴ concluded that

- a. When Fe^{2+} was present in excess over H_2O_2 , the reaction would be restricted to quantitative oxidation of Fe^{2+} by H_2O_2 ,



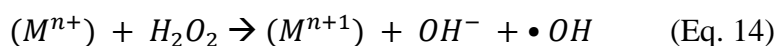
- b. When H_2O_2 was present in excess over Fe^{2+} , there was catalytic decomposition of H_2O_2 , and it accompanied the oxidation of Fe^{2+} ions,



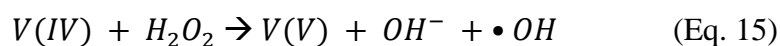
- c. The rate of reaction is of the first order with $[Fe^{2+}]$ and $[H_2O_2]$ at the beginning. However, the apparent order of the reaction increases with $[Fe^{2+}]$.

Although the Fenton reaction has been studied for over more than a hundred years, the exact mechanism has not been unanimously selected.

Similar to the reactions with ferrous salts, Fenton reactions could also involve other metal cations. The process is described as⁴⁵,



Such processes are described as “Fenton-like⁴⁶” mechanism where organic substrates are oxidized by a mixture of low-valent transition metal complex and hydrogen peroxide. Common examples⁴⁷ of such metals would be VO^{2+} , Ti^{3+} and Cr^{2+} . Vanadium, at physiological conditions, may produce hydroxyl radicals⁴⁸ -



1.6.2. TPA(terephthalic acid) Hydroxylation

The hydroxyl radicals can hydroxylate TPA molecule and form 2-hydroxy-terephthalic acid (2-OH-TPA) (**Figure 9**)⁴⁹. TPA hydroxylation is one of the most sensitive methods for detection of $\bullet OH$ radicals.

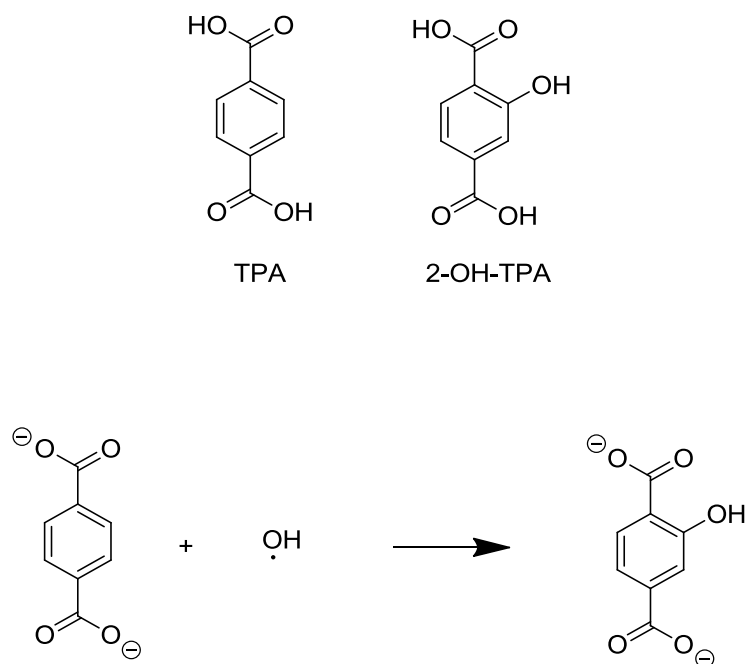


Figure 9. TPA hydroxylation.

Armstrong et al.,⁵⁰ used it as a replacement to calcium benzoate dosimeter and discovered it to be five to six times as sensitive as the benzoate dosimeter. Mason et al.,⁵¹ used TPA to assay radicals in sonochemistry. TPA itself is not fluorescent. However, the 2-OH-TPA (hydroxylated TPA) is fluorescence, the excitation wavelength being 315 nm and the emission wavelength being 425 nm⁵².

The hydroxylation reaction has been tested with Fenton reaction. The 2-OH-TPA was found to be stable for 24 h and the limit of detection for hydroxyl radical was determined to be 5nmol/L⁵³.

This project was aimed to couple the Fenton-like reaction with the hydroxylation of TPA (**Figure 10.** Fenton-like reaction coupled with TPA-hydroxylation.).

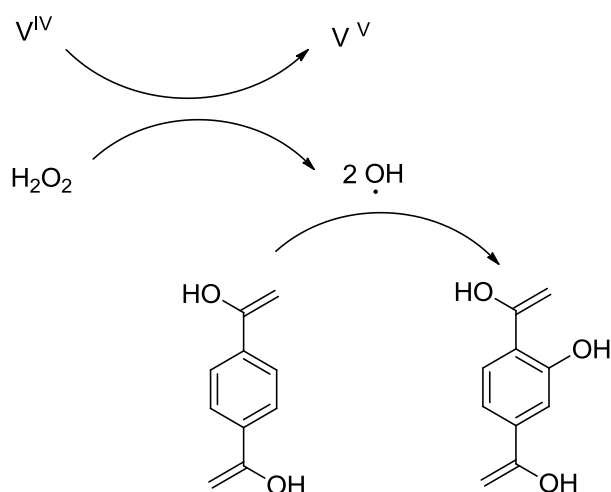


Figure 10. Fenton-like reaction coupled with TPA-hydroxylation.

1.7. Techniques used.

1.7.1. Agarose Gel Electrophoresis (AGE)

AGE is a very commonly used technique to determine the cleavage activity.

Plasmid DNA exists in 3 different forms (**Figure 2**). The different forms have different velocities in a medium of agarose gels under an electric potential. Since DNA has a phosphate backbone, it has a negative charge. At neutral pHs, the DNA is negatively charged. In the presence of an electric field, it moves towards the positive electrode. The movement of DNA depends on size and charge of the molecules. The larger the size of the molecules, the slower they move. The movement is directly proportional to the charge as well. It is assumed that the charge will remain constant after cleavage of plasmid DNA. The instrumental set-up of agarose gel electrophoresis is given in **Figure 11**.

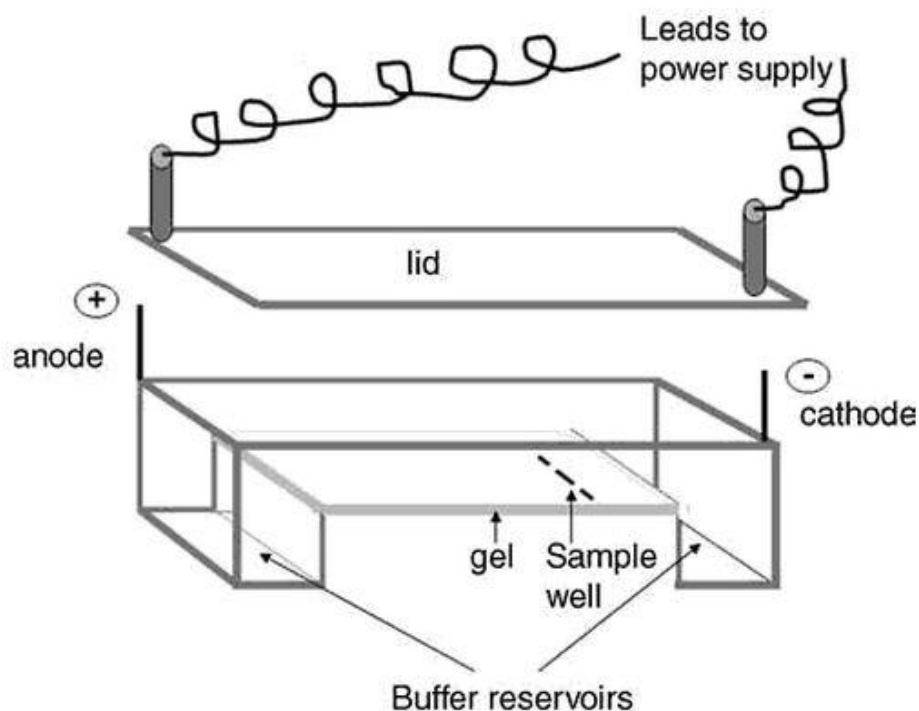


Figure 11. Instrumental set-up for AGE⁵⁴

Theoretical modeling has shown that under a uniform electric field, the movement of nucleic acid occurs in three formats-ogston sieving, reptation and rigid rods⁵⁵.

Ogston Sieving

This model explains that the nucleic acid molecules pass through the gel via formation of random globular molecules. The passage through the gel depends on the radius of gyration of the molecules. The fragments which have a radius of gyration smaller than the pores are able to pass through the gel quickly and the larger ones get blocked. However, these large molecules could switch from the globular molecules to other alternative conformations for passage through the pores.

Reptation

Under the influence of electric field, the nucleic acids, although present as globules, can enter the gel 'end on'. The movement through the gel occurs in a reptile like fashion. They move in a coiled and helical manner. The shorter molecules will pass quickly, but the larger ones will have to wind their way through the matrix and this separates the different fractions of nucleic acid.

Rigid Rods

At higher field strengths, the coiled/helical molecules begin to deform and migrate as rigid rods. However, the separating ability decreases under such conditions because the migration becomes size independent.

1.7.2. Absorption Spectrometry

When light of a certain wavelength irradiates a molecule, the molecules undergo a transition from a ground-state to an excited-state⁵⁶. The difference between the energy of the ground state electrons and the excited state electrons is the magnitude of the absorption. When a molecule absorbs energy, the transition that is most likely to take place is from HOMO (Highest Occupied Molecular Orbital) to LUMO (Lowest unoccupied molecular orbital). The greater the number of molecules capable of absorbing light of certain wavelength, the greater is the absorption.

When light at certain wavelength (λ) of intensity (I_0) enters a solution of concentration (c) in a cuvette, a part of light gets absorbed. (**Figure 12**)

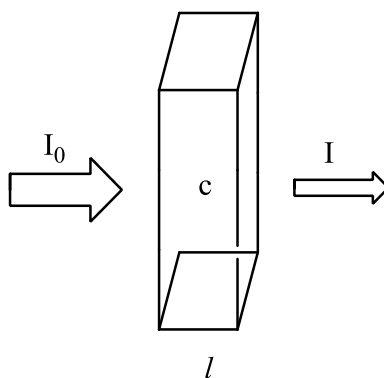


Figure 12. Light passing through a cuvette

The absorbance (A) is defined as

$$A = -\log (I/I_0) \quad (\text{Eq. 16})$$

According to Beer-lambert's law, the absorbance (A) is given as,

$$A = \epsilon l c \quad (\text{Eq. 17})$$

where ϵ is the molar absorptivity coefficient ($\text{mol}^{-1} \text{cm}^{-1}$) and l is the optical path length. This way, the absorption can be related with the concentration of the molecule being studied. The functioning of the double beam spectrophotometer is given in **Figure 13**⁵⁷.

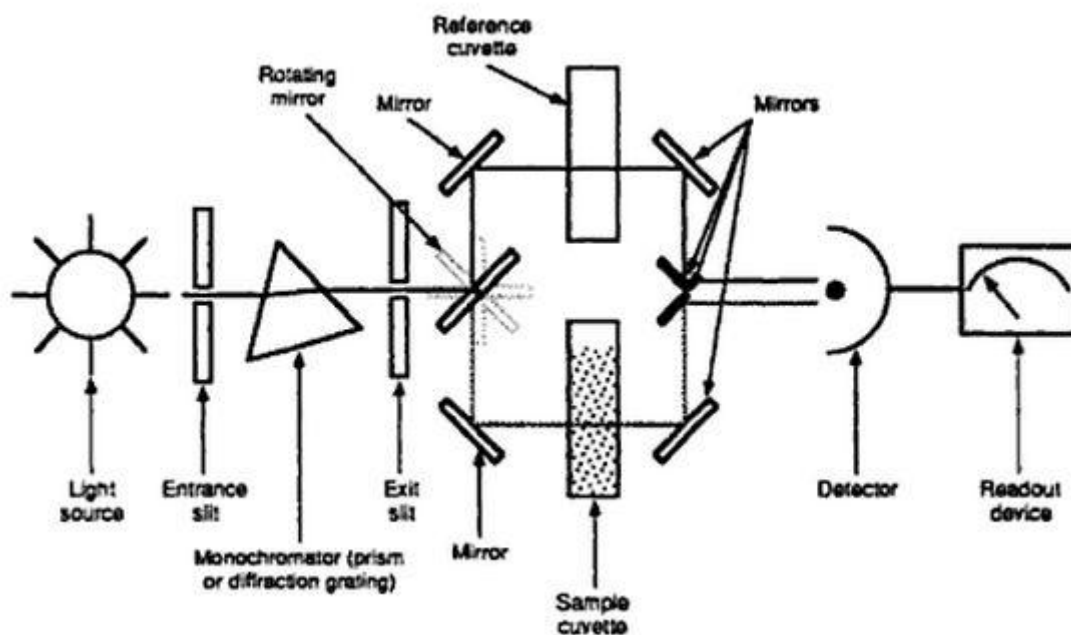


Figure 13. Schematic diagram of a spectrophotometer⁵⁷

Deuterium lamp is used as a light source. The monochromator provides the required wavelength. The rotating mirror is responsible for passing the light into the reference and the sample via mirrors. As a result, one beam of light passes through the reference, and another beam passes through the sample. The detector compares the electric circuitry between these two beams and thus the difference would depend on the absorbance of the light by the sample⁵⁸.

1.7.3. Fluorescence Spectroscopy

When a molecule absorbs a photon, it undergoes a transformation from ground level (S_0) to excited level ($S_n, n \geq 1$). An excited molecule will return to the ground level following successive steps⁵⁹. This is illustrated in Jablonski diagram in **Figure 14**.

Step 1. The molecule returns from S_n to its lowest excited level S_1 following energy dissipation into the surrounding environment.

Step 2. From S_1 , the molecule can return to S_0 via emission of a photon (fluorescence) with a radiative rate constant k_r . Other possible mechanisms are possible which are not discussed here. The lifetime of fluorescence lasts from 10^{-9} to 10^{-12} seconds. The lifetime of the fluorescence is affected by temperature, pressure, quenchers, and the different type of matrices used.

The spectrofluorometer is equipped with a Xenon lamp as a light source. The equipment (**Figure 15⁶⁰**) possesses two monochromators for selecting both the emission and excitation wavelength. The fluorescence is detected with photomultiplier tubes and quantified with appropriate electronic devices.

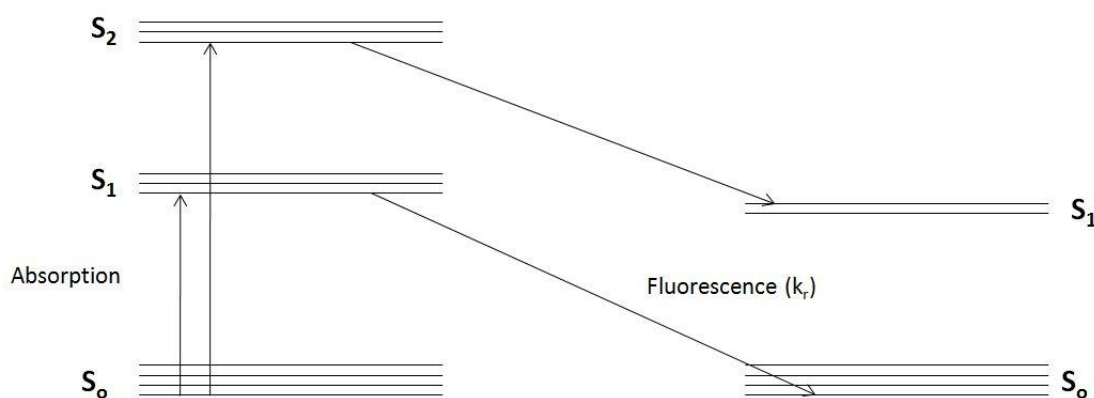


Figure 14. Jablonski Diagram illustrating the absorption and the emission processes.

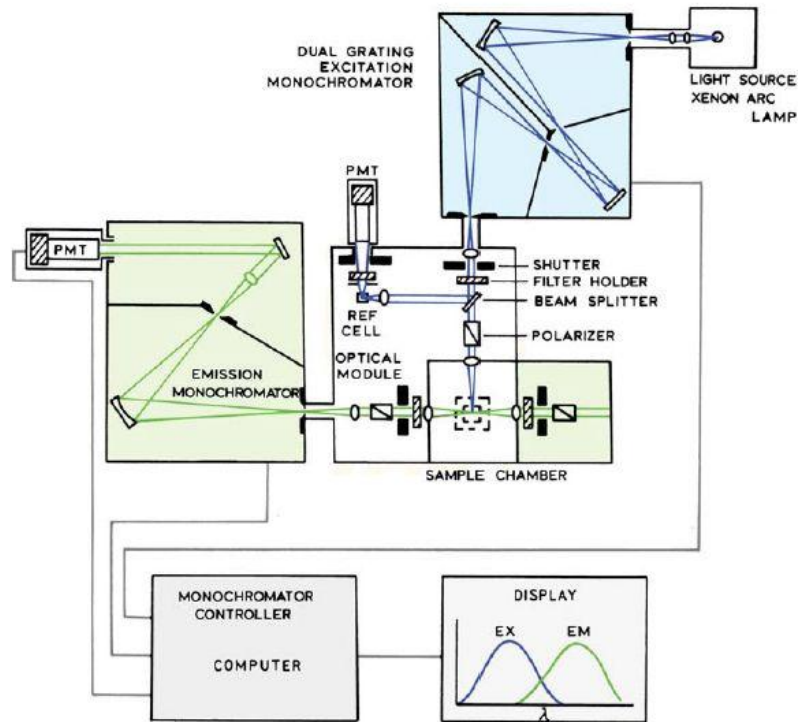


Figure 15. Schematic diagram of a spectrofluorometer⁶⁰.

1.8. Method validation parameters

1.8.1. LOD (limit of detection)

The LOD is the lowest concentration of analyte that the instrument can distinguish from against the blank/noise within a certain confidence interval (usually 95% intervals). Usually, it is determined by using the standard deviation (*sd*) of the blank sample. However, in this manuscript, the LOD is calculated using the least square methods.

$$LOD = \frac{3,3 \times sd_y}{m} \quad \text{Eq. 18.}$$

Where, sd_y is the standard error in the *y*-estimate and *m* is the slope.

1.8.2. Sensitivity

It is the ability of the instrument in a particular method to distinguish very small changes in concentration of the analyte. The slope (*m*) provides an estimation of sensitivity in this manuscript.

1.8.3. Precision

Precision in analytical method is the difference in the results when the same amount of analyte is used. The less difference in results there is for a certain concentration of analyte, the better the method is.

The precision in the analyte concentration is calculated in this manuscript. The standard deviation for the residuals, sd_y , obtained from the least squares linear regression can be used as an estimate of the precision of the method:

The standard deviation in output (sd_y) is given as,

$$sd_y = \sqrt{\frac{\sum(y-\hat{y})^2}{n-2}} \quad \text{Eq. 19}$$

Where,

n is the number of measurements and $\sum(y-\hat{y})^2$ is the sum of the squares of the residuals.

The standard deviation in the analyte concentration (sd_x) is given as,

$$sd_x = \frac{sd_y}{m} \quad \text{Eq. 20}$$

1.8.4. Estimation of errors

The estimation of errors (in the slope and the y-intercept) is performed using the t-student distribution at 95% confidence intervals. For example, the error in the slope (Δm) is given as,

$$\Delta m = t_{95\%(n-2)} \times sd_m \quad \text{Eq. 21}$$

2. Experimental Section

2.1. Instruments

A Shimadzu 1700 Pharmaspec UV-VIS absorption spectrophotometer was used to estimate the concentration of hydrogen peroxide. Three spectrofluorometers (Fluoromax 3 and Fluoromax 4, Horiba and Jasco FP-777) were used to study the fluorescence of TPA-OH that was formed during the course of the reaction. The software used to operate the Horiba spectrofluorimeters was FluorEssence v3.5

A 1 cm quartz crystal cuvette (Sigma Aldrich) was used to measure the fluorescence.

AlphaImager from Alpha Innotech was used for capturing the gel images. AlphaEaseFC was the software used to operate the instrument.

2.2. Preparation of solutions

2.2.1. Phosphate buffer:

A solution of K_2HPO_4 (Panreac, 99%) was made by dissolving 50 mmoles of K_2HPO_4 in 500 mL water. The pH of the solution was adjusted to 7,4 by the addition of concentrated HNO_3 (Merck, 65%). The solution was then stored in the refrigerator for further use.

2.2.2. TPA(Terephthalic acid) solution

The TPA solution was made by dissolving 66 mg TPA (Sigma Aldrich, 95%) in 20mM Phosphate buffer.

2.2.3. Concentrated TBE solution

A solution of 101,81 g Trizma base(Sigma Aldrich, 99%), 55,029 g Boric acid(Riedel de Häen, 99,5%) and 7.776 g of EDTA(analaR, 99,5%) were dissolved in 1,0 L of water. The pH was measured (~8,0) and kept in the refrigerator for further use. The solution was labeled 10X TBE. Further dilutions were made when necessary.

2.2.4. Water

In all cases, Millipore water (resistivity > 18M Ω .cm) was used, unless otherwise mentioned.

2.2.5. Vanadium complexes solution

Different solutions of VOSO₄, VO(acac) and VO(clor) were made by dissolving respective concentrations of complexes in water.

2.2.6. Hydrogen Peroxide

Water was used to dilute the original hydrogen peroxide (Sigma Aldrich and BDH Prolab , 30%) into required concentration amounts. The concentration of peroxide was estimated using absorbance measurements⁶¹.

$$\varepsilon = 74\text{M}^{-1}\text{cm}^{-1}$$

2.3. **Spectrofluorimetric measurements**

2.3.1. Preparation of solutions

A solution of 400 μM TPA was prepared in 20 mM phosphate buffer. 10 mL of this solution was poured into a 20,0 mL volumetric flask. A certain volume of vanadium complex [VO(acac)₂ (Sigma Aldrich, 98%) or VOSO₄ (Aldrich)] solution depending on the concentration needed was added and water was used to fill upto the 20 mL mark. 10 mL of this solution (final concentrations : 200 μM TPA, 10 mM phosphate buffer and 0-100 μM of vanadium complex) was added to another beaker.

In later experiments with galactose, necessary amount of galactose (Koch-Light, pure) was added to the solution of TPA. The solutions were made of 0,050 % (0,05 g galactose in 100 mL solution), 0,25% and 0,50%.

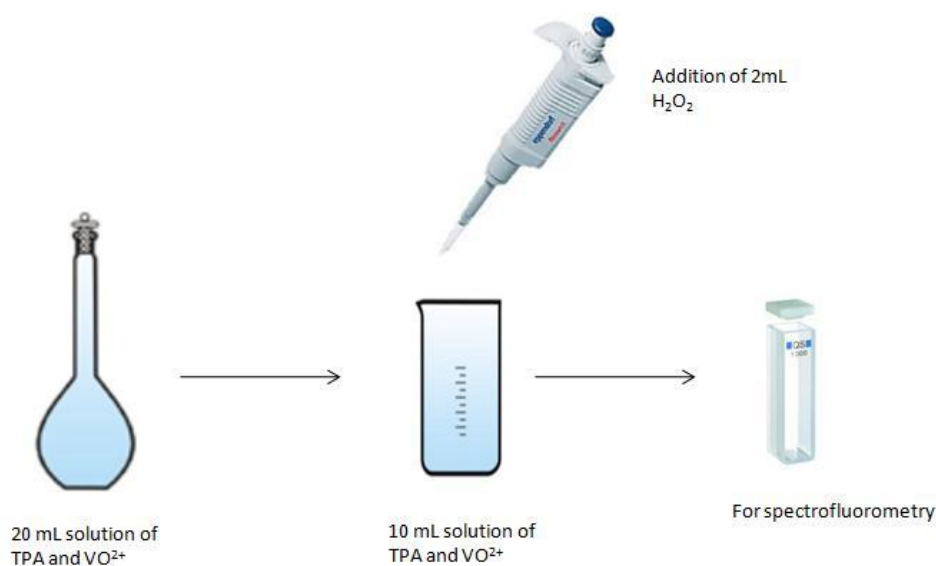


Figure 16. Procedure of spectrofluorimetric measurement

2.3.2. Fluorescence measurement

The excitation wavelength was 312 nm and the emission was monitored from 350 nm to 500 nm. The slit wavelength was 1 nm (excitation and emission slits) for the measurements in aqueous solutions and 2 nm (for both the excitation and the emission slits) in solutions with galactose concentration higher than 0,050% or with agarose gels. The integration time was set 1 nm/s for Fluoromax 3, and 0,1 nm/s for Fluoromax 4. These integration times were *default settings* of the instrument.

The fluorescence was measured after 45 seconds (timed 0 minute) of addition of H_2O_2 to the TPA/Vanadium solution, 5 minute 45 seconds (timed 5 minutes) and so on until 20 minutes.

When the data contained large levels of noise (observed in presence of galactose), the smoothening was performed using Savitzky-Golay algorithm(10 points of window, 2 degree polynomial).

2.4. Agarose gel preparation.

2.4.1. Agarose Gel Electrophoresis

2.4.1.1. *Plasmid DNA*

pA1 plasmid DNA[consisting of full-length cDNA from Cytochrome P450 CYP3A1 inserted in the PBS plasmid vector(pBluescribe, Stratagene, UK)]^{Error! Bookmark not defined.} prepared by Nataliya Butenko was used for gel electrophoresis experiments. The linear DNA(also prepared by Nataliya) was obtained by digesting of pA1 with HINDIII and was used as a reference in agarose gel electrophoresis.

2.4.1.2. *DNA cleavage activity*

The cleavage activity of DNA was studied by the transformation of the supercoiled plasmid DNA (Sc) to nicked circular and linear DNA. The reaction mixture was prepared by addition (in this order) 6 μL of water, 2 μL (0.2 μg) of supercoiled pA1 DNA, 2 μL of 100 mM K_2HPO_4 buffer (pH 7,4) and 10 μL of the aqueous solution of the vanadium complex [$\text{VO}(\text{acac})_2$ –Sigma Aldrich, 98% purity) and VO(clor) (sample from Prof. Susana Etcheverry)].

Before gel electrophoresis, the samples were wrapped up in aluminum foil were incubated for 1 h at 37^0C . After incubation, 5 μL of loading buffer (0.25% bromophenol blue, 0.25% xylene cyanol, 30% glycerol in water), were added to the samples and the solutions were loaded onto a 1% agarose gel containing ethidium bromide (EtBr). Non-incubated and linearized plasmid DNA was used in the extremes of 18 well gel for control purposes. The electrophoresis was done at 110 V for 3 h. The bands were then photographed under UV light using AlphaImager.

2.4.2. Agarose gels for testing the Fenton-like reaction coupling with TPA hydroxylation.

To a dissolved solution of 200 μ M TPA (Sigma Aldrich, 99%) in 150 mL of 0,50X TBE, 1,5 g of agarose was added. The solution was then microwave- heated until the agarose dissolved. When the solution cooled down, it was poured in a gel holder to facilitate the solidification.

In one of the experiments, a very concentrated (saturated) and a 100 μ M sample of VO_2SO_4 and H_2O_2 were added while the gel was solidifying. Water was used as a control. It was taken care that the tip of the pipette did not touch the gel solution during addition.

Marks were made on a side by the use of pipette-tips. The schematic diagram of the gel is given in (**Figure 17**). The illumination was performed with UV light of 302 nm.

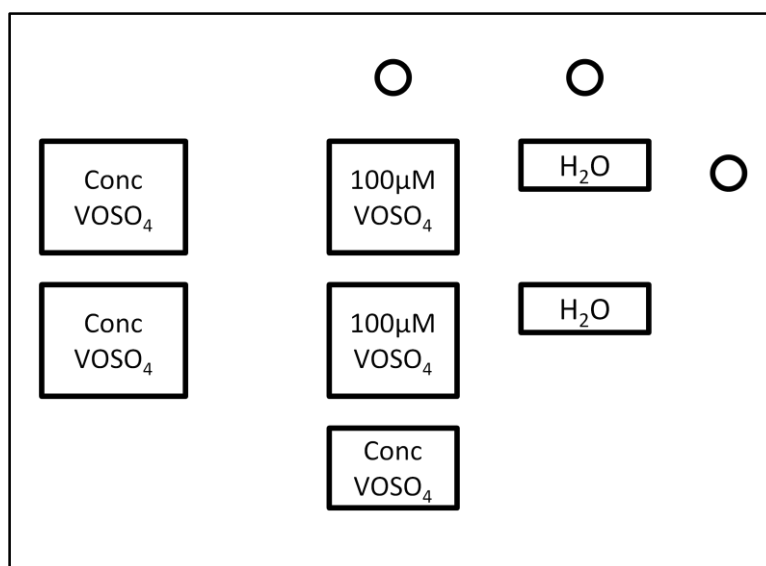


Figure 17. The position of samples of vanadium in 1% agarose gel containing 200 μ M TPA.

2.4.3. Agarose gels in cuvette

To study the fluorescence in gels, agarose gel was prepared with TPA and VO(acac)₂ and H₂O₂.

2.4.3.1. *Boiling and dissolving agarose only with TPA.*

A solution (**Solution 1**) of 0,0066 g (400 μmol) TPA and 2,0g (2%) agarose were added to a solution of 50 mL 40 mM phosphate buffer and 50 mL 2X TBE. In another flask, a solution (**Solution 2**) of 0,0159 g (600 μmol) VO(acac)₂ was prepared. A solution of hydrogen peroxide (1,6 mM) was prepared as well.

Solution 1 was heated until agarose dissolved. 1,0 mL of this solution was added to a cuvette where 1,0 mL of **Solution 2** and 0,4 mL of peroxide were already added. In another cuvette, 1,0 mL of heated **Solution 1** was added followed by 1,0 mL of **Solution 2** and 0,4 mL of hydrogen peroxide solution.

2.4.3.2. *Boiling and dissolving agarose with TPA, VO(acac)₂ and H₂O₂*

A solution of 0,0034 g TPA (200 μmol), 0,0079 g VO(acac)₂ (300 μmol), 1,0 g agarose (1%) were added in a 100 mL volumetric flask. The vanadium complex was not added for blank measurements. Instead, water was used. Also added was 4,0 mL 10X TBE, 10,0 mL of 100 mM phosphate buffer and the water was used to fill upto the mark. The solution was then added to another beaker and 15,0 mL of 1,8 mM H₂O₂ was added and left for 30 minutes. The solution was then heated until the agarose dissolved. When the temperature of the solution was ~80°C, the solution was added to a cuvette and left for solidification and later fluorescence measurements were performed.

3. Results and Discussion

3.1. Agarose gel electrophoresis

The result from one agarose gel electrophoresis is given in **Figure 8** .

It can be observed that both VO(acac)₂ and VO(Cl₂) cleave DNA. There is presence of linear and nicked bands in the samples containing vanadium complexes but not in the control sample. The band intensity of supercoiled DNA decreases with increasing concentration of VO(acac)₂ and the band intensity of the nicked and linear DNA increase with increasing concentration.

3.2. Preliminary tests in agarose gel.

The results of the gel imaging with Vanadium is given in (**Figure 18**)

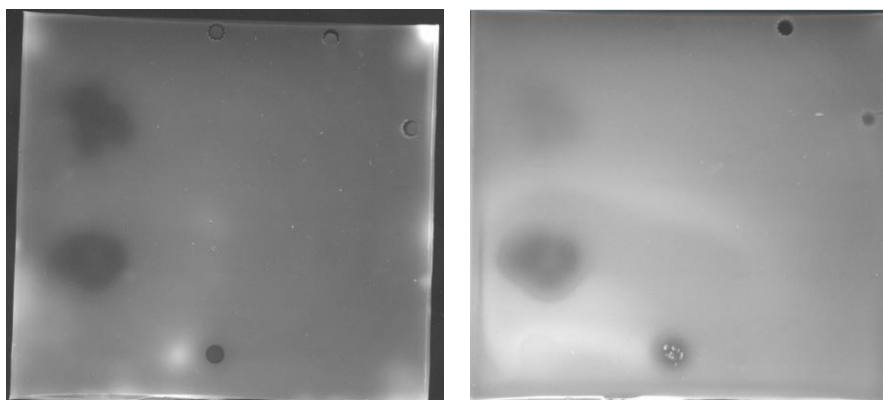


Figure 18. Gel imaging of experiment from **Figure 17** before addition of H₂O₂ (left) and after addition of H₂O₂ (right). [Excitation at 302 nm and filter at (595 ± 40) nm]

The spots that contained VOSO₄ (conc) appeared as dark spots on the image. At lower concentrations of VOSO₄, no such spots were observed. The dark spots (on the left in **Figure 18**. Gel imaging of experiment from **Figure 17** before addition of H₂O₂) can be attributed to the precipitation of vanadium hydroxides. An interesting observation was that after the addition of peroxide, large bright spots appeared in the gel. This could be due to fluorescence of 2-OH-TPA formed by the reaction of TPA with .OH generated

by H_2O_2 in contact with the gel. The maximum for the emission of 2-OH-TPA occurs at 425 nm, a lower wavelength lower than the (595 ± 40) nm imaging system filter window. The bright areas were probably due to diffraction in the gel caused by surface changes in the gel. Using this method would require acquiring a different filter of (464 ± 40) nm for the imaging system.

3.3. TPA-hydroxylation coupled with Fenton-like reactions

3.3.1. Method development in aqueous solutions.

Experiments with TPA-hydroxylation with Fenton-like reaction using $\text{VO}(\text{acac})_2/\text{VOSO}_4$ were done. The concentration of the Vanadium complexes were varied from 0-100 μM and H_2O_2 was added in a large excess ($\sim 9,0$ M). The fluorescence emission spectra were measured every 5 minutes upto 60 minutes. The results can be seen in **Figure 19** and **Figure 20**.

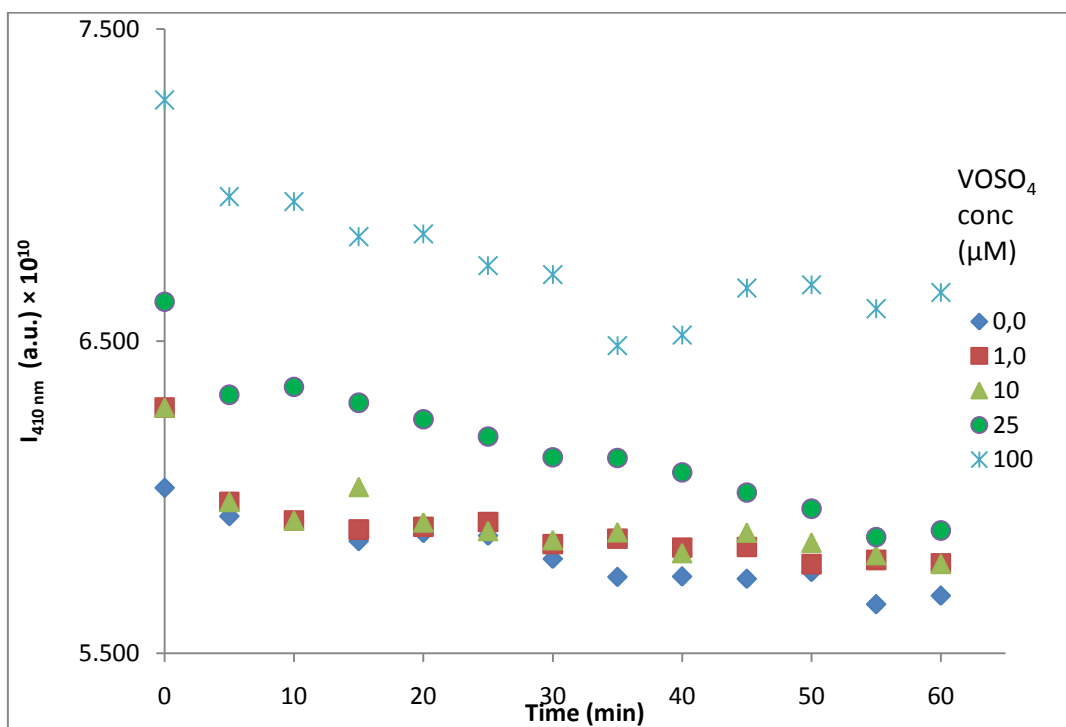


Figure 19. Time evolution of maximum intensity (410 nm) of 2-OH-TPA generated from different concentrations of VOSO_4 over time. $\text{H}_2\text{O}_{2\text{conc}} = (\sim 9\text{M})$

It was expected that the fluorescence intensity should increase over time due to the increase in formation of 2-OH-TPA. However, this was not the case in this experiment. A particular example can be seen in that **Figure 21**. The intensity decreases as a function of time regardless of the concentration of vanadium complex used.

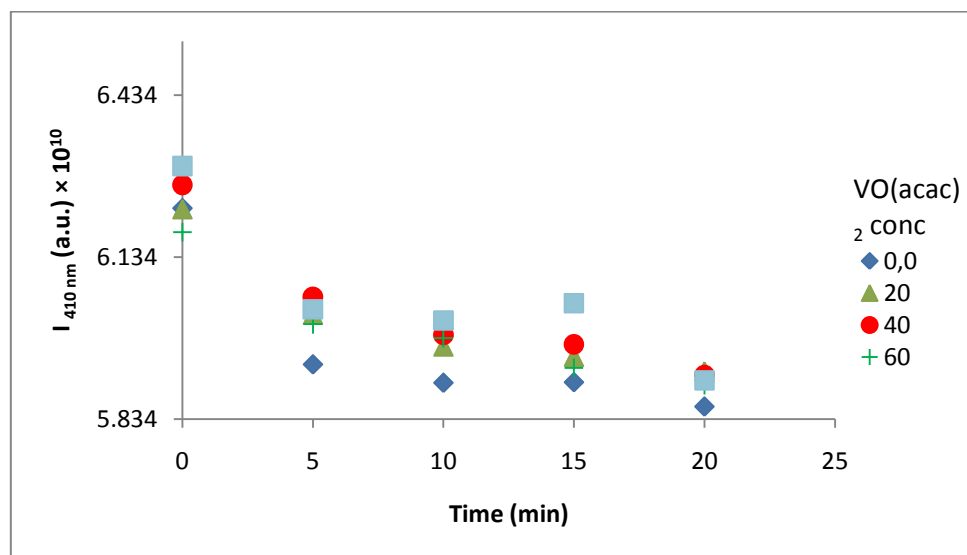


Figure 20. Time evolution of maximum intensity (410 nm) of 2-OH-TPA generated from different concentrations of VO(acac)₂ over time. H₂O₂_{conc} = (~9M)

A possible explanation is that the reaction between •OH and TPA provides a mono-hydroxylated compound and the further hydroxylation is negligible only under the conditions when the concentration of TPA is much higher than the concentration of hydroxide radicals⁵³. When the concentration of •OH is higher than the concentration of TPA conditions, hydroxylation could have taken place in one or more carbon atoms than the ortho position (**Figure 22**).

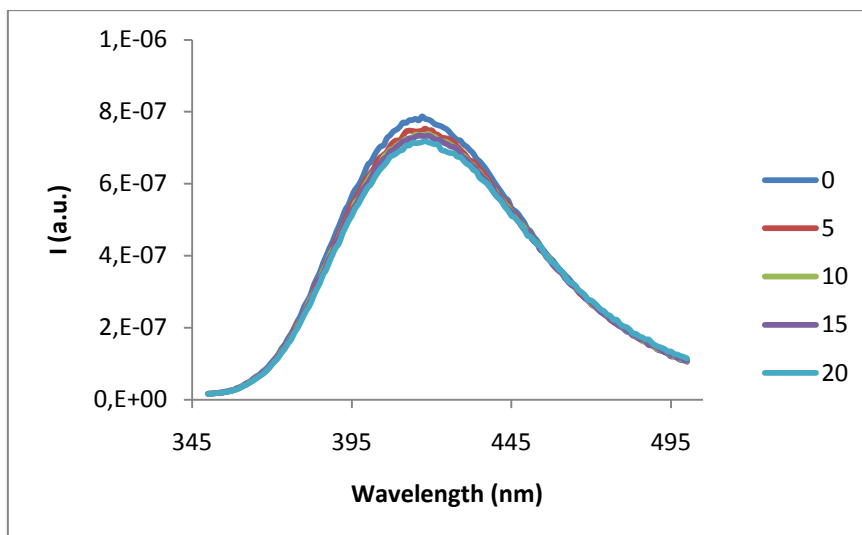


Figure 21. Fluorescence spectra measurements for 80 μ M VO(acac)₂ over time.
H₂O_{2conc} = ~9M

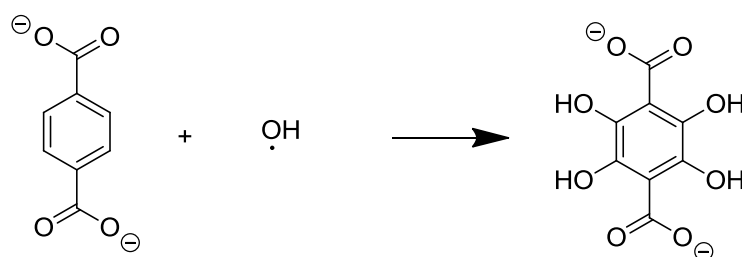


Figure 22. Figure showing the different positions in the benzene ring where hydroxylation can take place when large excess of .OH radicals are present.

A low concentration of H₂O₂ was used in the further experiments. When the concentration of H₂O₂ used was 1,8 mM, the intensity of 2-OH-TPA in the solution increased with time for all concentrations except blank. The results can be seen in **Figure 23** and **Figure 24**.

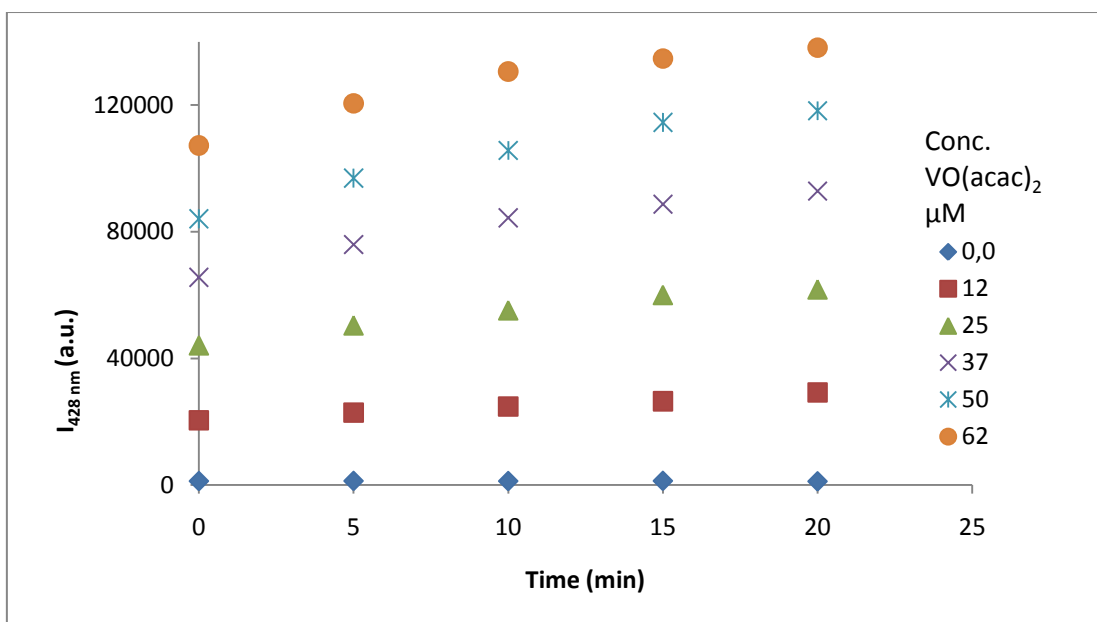


Figure 23. Time evolution of maximum intensity (428 nm) of 2-OH-TPA generated from concentrations of $\text{VO}(\text{acac})_4$ over time. $\text{H}_2\text{O}_{2\text{conc}} = 1,8\text{M}$

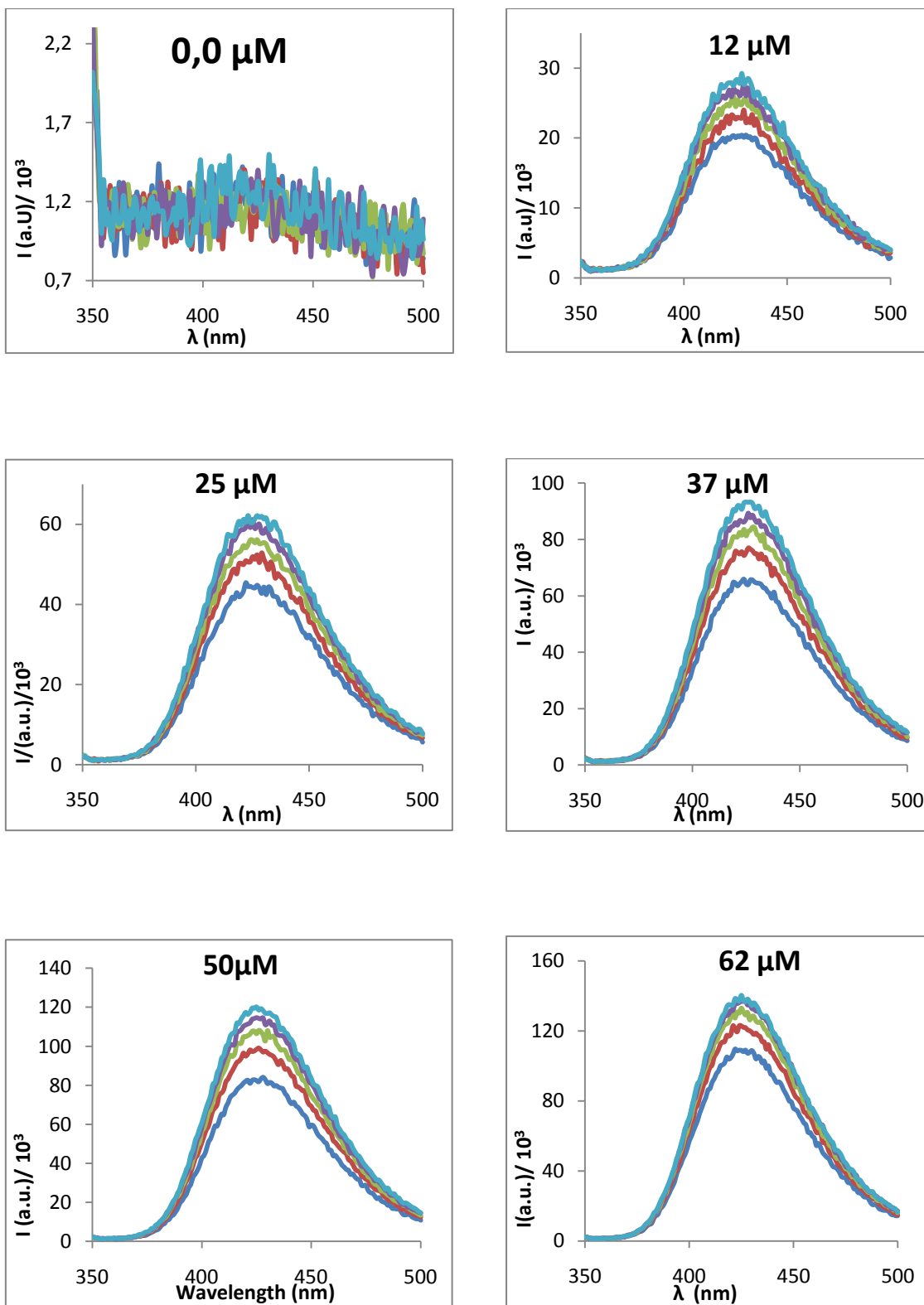


Figure 24. Individual fluorescence spectrum measurements for different concentrations of $\text{VO}(\text{acac})_2$. $\text{H}_2\text{O}_{2\text{conc}} = 1,8 \text{ mM}$.



It can be seen that in **Figure 23**, the intensity of the formed 2-OH-TPA species in the solution increases slightly over time during a course of 20 min. The increase is related to increase in the number of fluorescent species, i.e., 2-OH-TPA. There was no increase in intensity observed for the blank solution.

The next step was to develop a relation between the concentration of Vanadium used and the fluorescence produced. So, a graph between amount of fluorescence and the concentration of vanadium used was made in **Figure 25**.

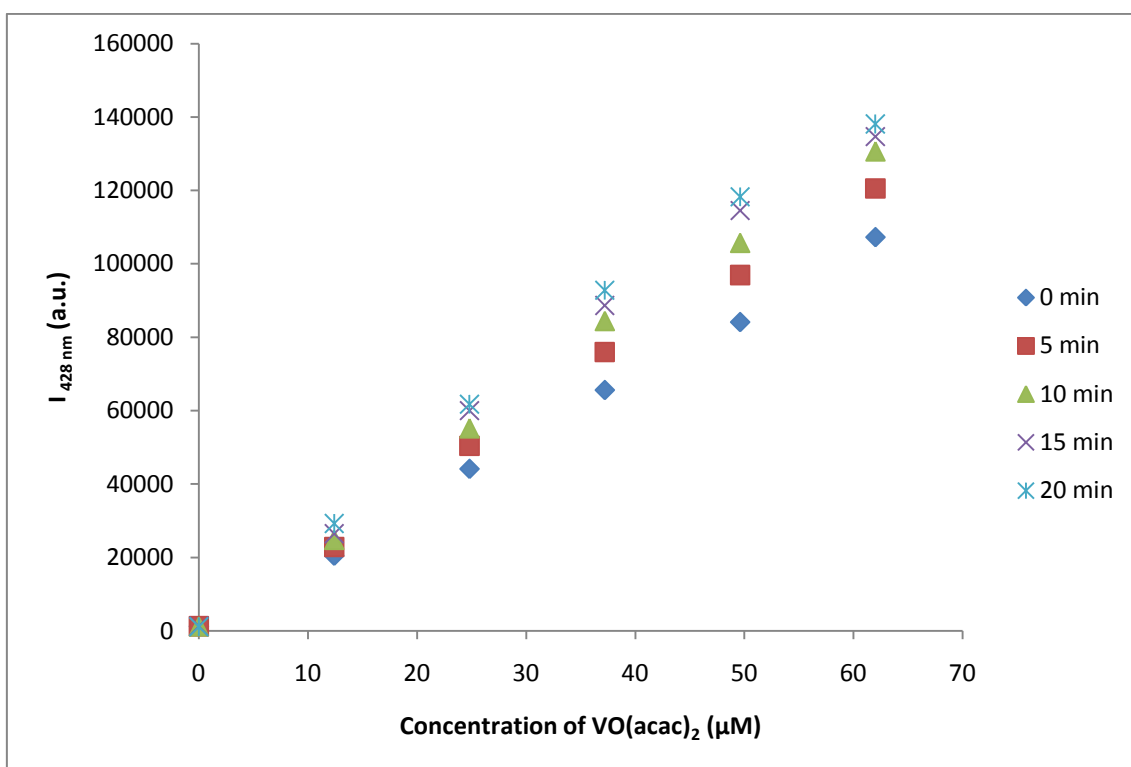


Figure 25. Maximum intensity (428nm) of 2-OH-TPA with different concentrations of VO(acac)₂ over time. H₂O_{2conc} = 1,8 mM

To optimize the particular time period, sensitivity was checked at different time intervals. A rough estimation of the precision in the concentrations was also performed. The results are given in **Table 1**.

Table 1. Parameters to study the sensitivity at different time intervals for TPA hydroxylation coupled to Fenton-like reactions. The errors are presented with 95% confidence intervals

Time (t) (min)	Slope (m)/(10 ³) (a.u./μM)	y-intercept (b)/ (10 ³) (a.u.)	Standard deviation (sd _x) (μM)
0	1,70 ± 0,11	0,73 ± 4,2	0,8
5	1,90 ± 0,16	1,0 ± 6,0	1,0
10	2,10 ± 0,24	1,3 ± 8,9	1,3
15	2,20 ± 0,34	2,4 ± 13	1,8
20	2,30 ± 0,37	3,4 ± 14	2,0

At time 0, the sensitivity is significantly less compared to time 10 minutes or above. However, at times 10 minutes or above, the errors in the slope, y-intercept and CV_x are higher. At time 5 minutes, the sensitivity is not significantly different from other time intervals. Therefore, time 5 minutes would be the most favorable time to measure the fluorescence of the 2-OH-TPA species formed in the samples. LOD for time period 5 minutes was calculated to be 4,1 μM from the calibration curve.

The equation for the line at 5 minutes are given as,

$$y = (1,90 \pm 0,16) \times 10^3 x + (1,0 \pm 6,0) \times 10^3 \quad \text{Eq. 22}$$

3.3.2. With D-galactose

The next step of the method was to try it in agarose. The problem with agarose is that agarose has to be heated to solidify into gels. It was decided that the system should first be used in galactose. Galactose would provide a very close resemblance to agarose in terms of matrix composition and is easily soluble. Therefore, in the further experiments, increasing concentrations of galactose were added to the TPA solutions.

An initial set of measurements were done with 0,050%, 0,25% and 0,50% D-galactose. The peroxide concentration used was estimated to be 1,8 mM and the data was treated with Savitzky-Golay smoothing.

With the presence of galactose, the fluorescence was lower (the maximum value ~25k units with 110 μM VO(acac)₂ (**Figure 26**) compared to ~130k for 62 μM VO(acac)₂ (**Figure 23** and **Figure 24**).

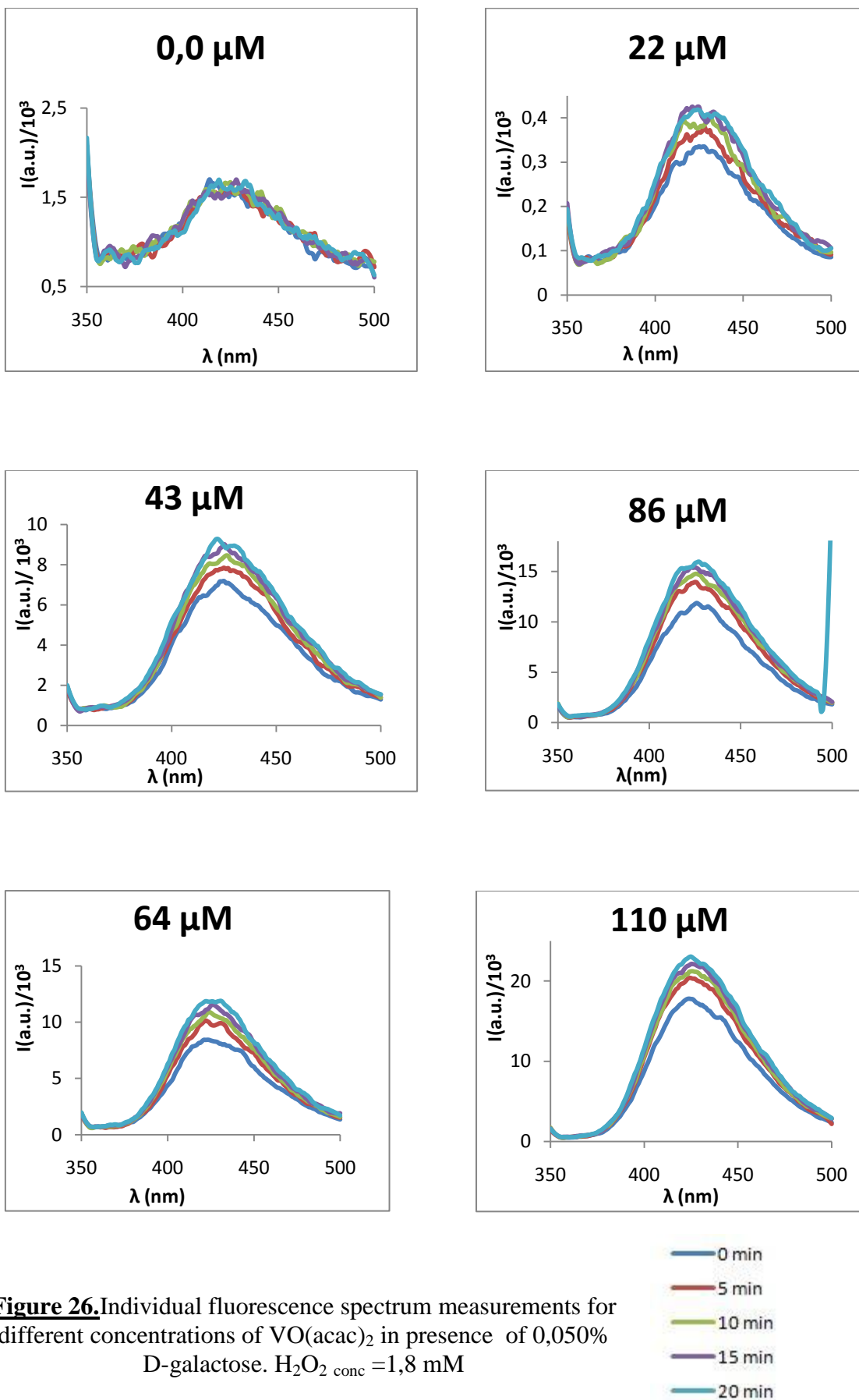


Figure 26. Individual fluorescence spectrum measurements for different concentrations of $\text{VO}(\text{acac})_2$ in presence of 0,050% D-galactose. H_2O_2 conc = 1,8 mM

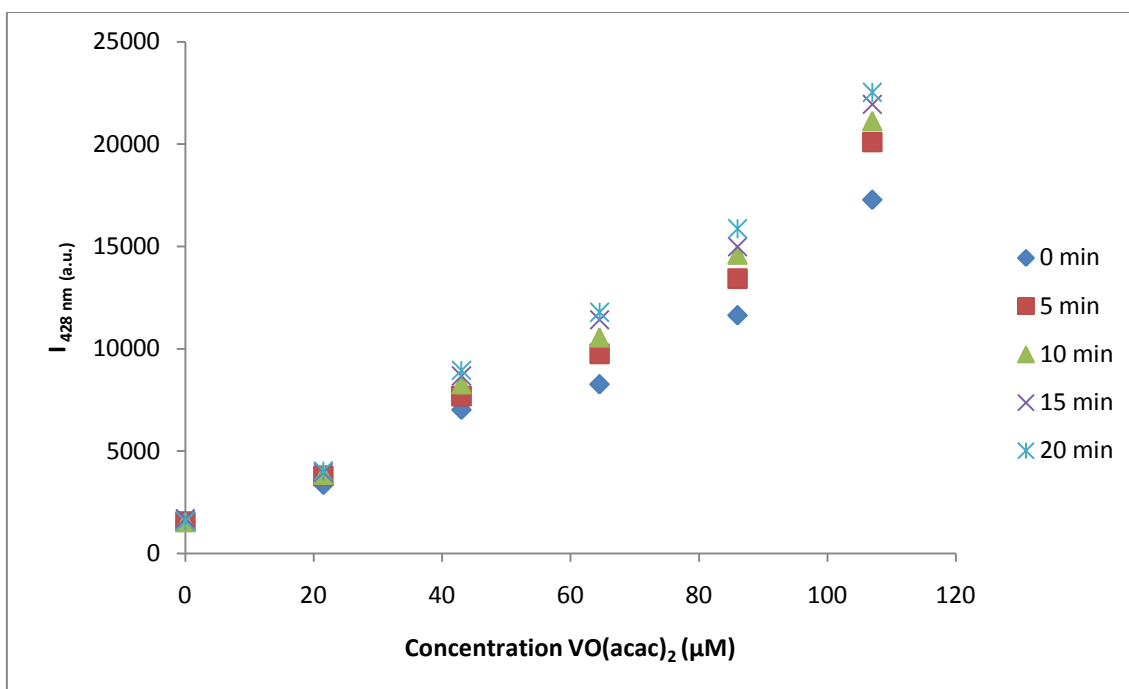


Figure 27. Maximum intensity (428nm) of 2-OH-TPA generated from different concentrations of VO(acac)₂ over time. H₂O_{2conc} = 1,8 mM, galactose= 0,050%.

It can be observed from **Figure 27** that the maximum intensity of the formed 2-OH-TPA species increased with concentrations in a linear fashion. The galactose concentration was then increased from 0,050% to 0,50%. At 0,50%, a working range was studied. The study is shown in **Figure 28** and **Figure 29**. The peroxide concentration used for this experiment were 1,9 mM for VO(acac)₂ and 1,8 mM for VOSO₄ respectively. It can be observed that at concentrations of 0-300 μM of vanadium complexes, the fluorescence increased in a linear fashion. However, at higher concentrations the fluorescence intensity remained constant or decreased. It is a possibility that that the complexes precipitated at higher concentrations.

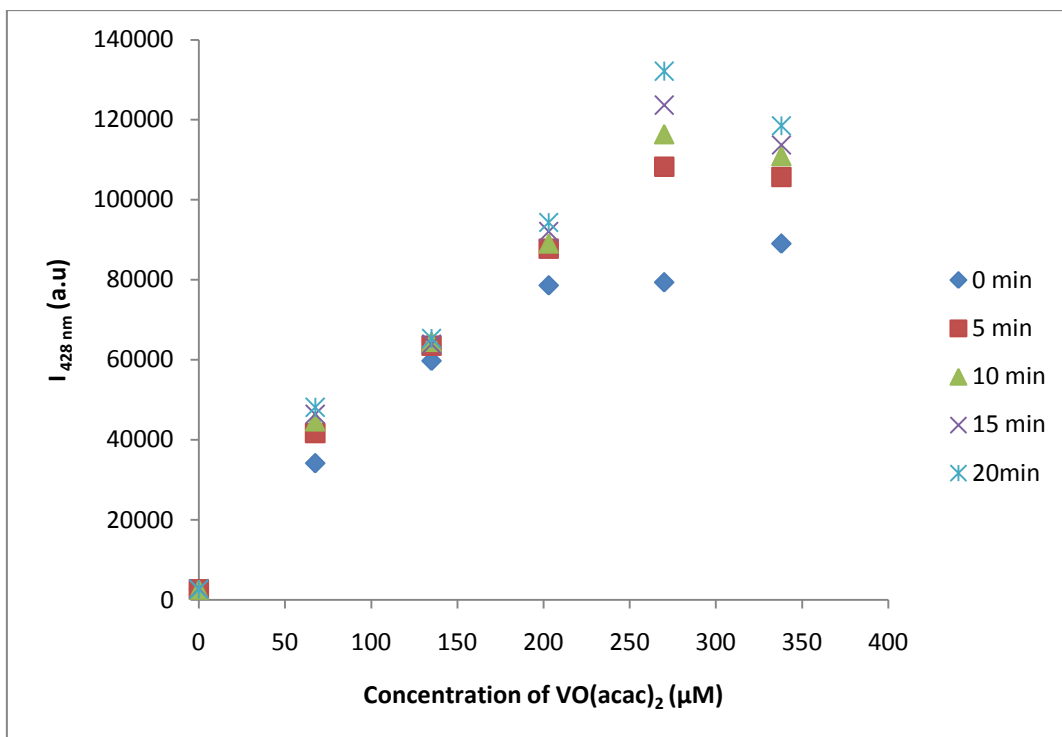


Figure 28. Maximum intensity (428nm) of 2-OH-TPA generated from different concentrations of VO(acac)₂ over time. H₂O_{2conc} = 1,9 mM, galactose= 0,50%.

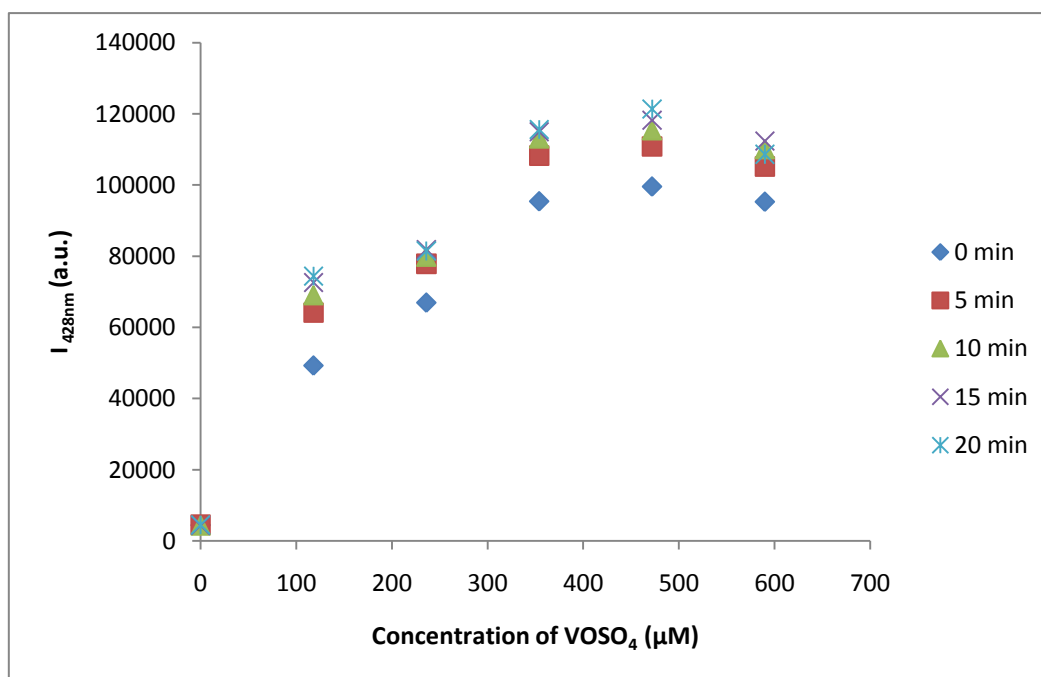


Figure 29. Maximum intensity (428nm) of 2-OH-TPA generated from different concentrations of VOSO₄ over time. H₂O_{2conc} = 1,8 mM, galactose= 0,50%.

The next steps were to determine the LOD (Limit of Detection) in presence of 0,50% galactose. Concentrations of as low as 2,0 μM and the highest 83 μM were used. The concentration of peroxide used was estimated to be 1,9 mM. The relationship between the concentrations and the fluorescence is given in **Figure 30**.

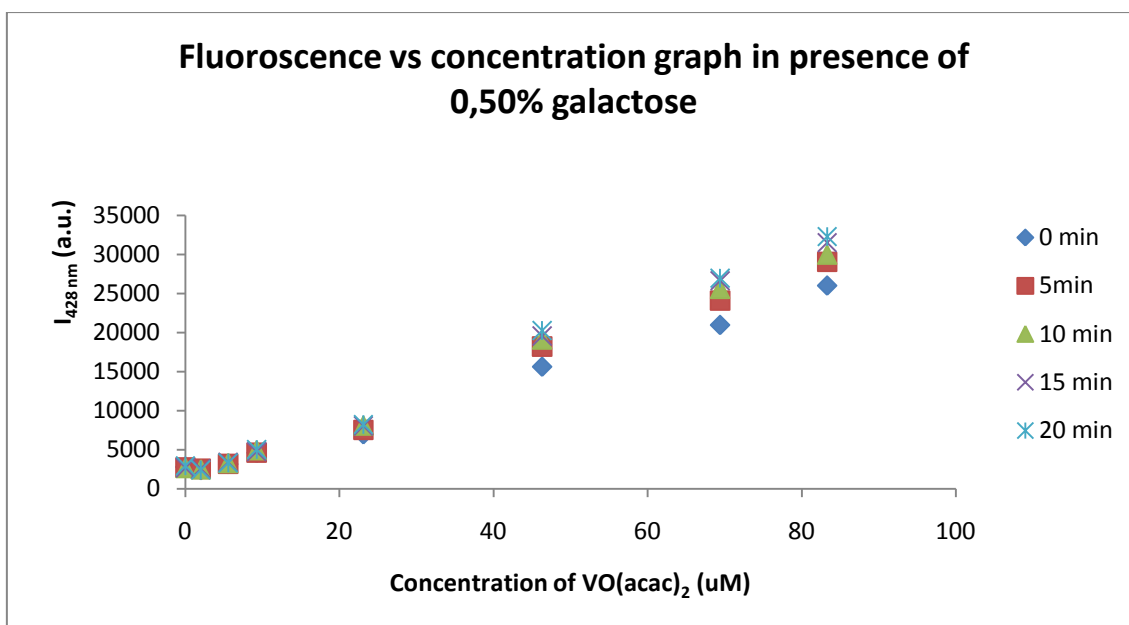


Figure 30. Maximum intensity (428nm) of 2-OH-TPA generated from different concentrations of VO(acac)₂ over time. H₂O_{2conc} = 1,9 mM, galactose= 0,50%.

Least squares method was used to calculate the LOD. 4 lowest concentrations were taken for a better estimate of LOD.

A comparison between the different galactose concentrations and the sensitivities (at 5 minutes) for VO(acac)₂ was performed, the results of which are given in **Table 2**.

Table 2. A comparison (at 5 min) between the sensitivities when different wt% of galactose was used. The values are presented with 95% confidence intervals.

Galactose (wt %) (g/100mL)	Slitwidth (nm)	Slope (m)/(10 ³) (a.u./ μM)	y-intercept/ (10 ³) (b) (a.u.)	Standard deviation(sd _x) (μM)	Standard deviation(sd _x) (μM)	Range (μM)
0,0	1	1,9 ± 0,2	1,0 ± 6,0	1,0	1,0	0-62
0,050	1	0,17 ± 0,07	0,5 ± 4,5	8,8	8,8	0-107
0,49	2	0,33 ± 0,03	1,7 ± 1,2	3,0	3,0	0-83

The slope without the presence of galactose is higher (1900 ± 160) a.u./ μM whereas, for 0,050% of galactose is (170 ± 70) a.u./ μM . The change in the sensitivity is significant at 95% confidence intervals. The precision is lower when galactose is used. (CV_x for 0,050% galactose is 8,8 μM whereas for 0,0% galactose is 1,0 μM).

The lowering of the sensitivity and the precision could be because the presence of galactose interferes with the fluorescent species (2-OH-TPA). Or, perhaps, galactose, in high concentration, will act as a radical scavenger and decrease the concentration of hydroxyl radicals available to react with TPA. However, with increasing slitwidth increases the sensitivity significantly. With the use of 0,50% galactose and 2 nm slitwidth, the slope obtained was (330 ± 28) a.u./ μM . whereas with the use of 0,050% galactose and 1 nm slitwidth, the slope obtained was (170 ± 70) a.u./ μM . the precision is also better when slitwidth is increased($\text{CV}_x= 8,8 \mu\text{M}$ for 0,050% and 3,0 for 0,50%)

3.4. Fluorescence in agarose gels

This would theoretically be the part of the experiment where one could determine if the methodology functions. The main aim of the experiments was to transform the hydroxylation of TPA coupled to Fenton-like mechanism from an aqueous medium to agarose gels.

3.4.1. Boiling and dissolving agarose only with TPA

As the agarose/TPA solution was warm and the Vanadium solution is cold, a homogeneous solution was difficult to achieve. Without a homogenous sample, the results obtained from fluorescence spectrofluorometry are inconclusive because there exists numerous light scattering effects. Thus, another approach of boiling all components of agarose gel-agarose, TPA, H_2O_2 and $\text{VO}(\text{acac})_2$ together was pursued.

3.4.2. Boiling and dissolving agarose with TPA, $\text{VO}(\text{acac})_2$ and H_2O_2

TPA, $\text{VO}(\text{acac})_2$, agarose and H_2O_2 were mixed in one beaker and heated until agarose dissolved. The sample was added in a cuvette and taken for fluorescence after solidification. The result is given in **Figure 31**. Fluorescence spectra measurement of 1% agarose gels containing 200 μM TPA and 1,8 mM H_2O_2 ..

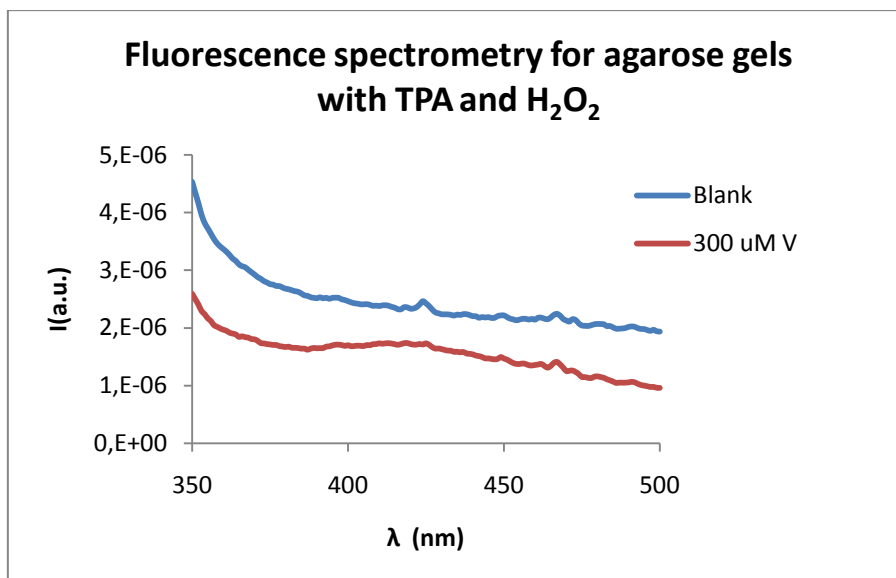


Figure 31. Fluorescence spectra measurement of 1% agarose gels containing 200 μ M TPA and 1,8 mM H₂O₂.

It can be observed that in **Figure 31**, the fluorescence with 300 μ M VO(acac)₂ is lower than the blank. However, one particular aspect to notice is that for the spectra with Vanadium, there appears a hump near from approximately 395 to 440 nm. This is very similar with the spectra that were obtained for 2-OH-TPA. No such hump can be observed with the blank sample. The intensity at 428 nm is not very high and it could have resulted from poly-hydroxylation of TPA or the degradation of 2-TPA during the heating or the suppression of the fluorescence by agarose gels.

3.5. Stability of Hydrogen Peroxide

As H_2O_2 is a very good oxidizing agent. Due to its oxidizing nature, this compound is not very stable. Therefore, the concentration of peroxide was an important factor to monitor. Various dilution factors were made and the absorbance measurements were performed over a time of 6 hours (the usual time of an experiment).

The results are shown in **Figure 32**.

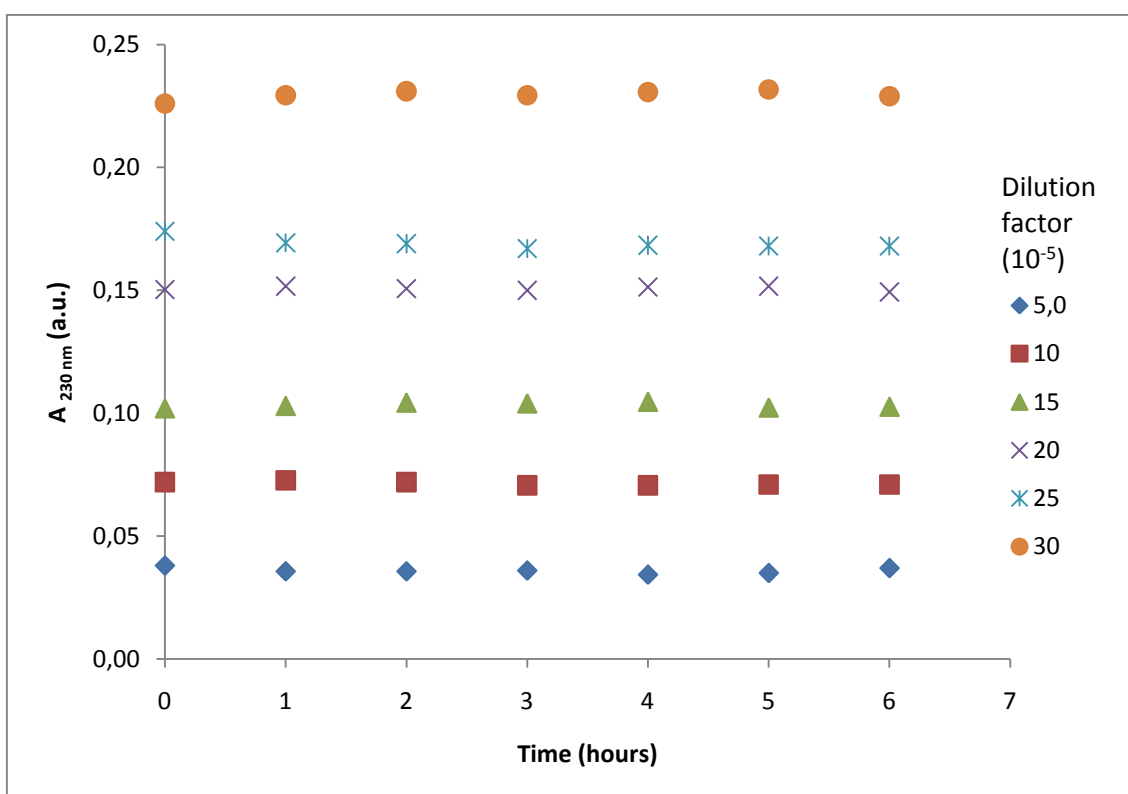


Figure 32. Absorbance of hydrogen peroxide over time.

There was no significant change observed during a period of 6 hours and thus it can be concluded that the experimental data was not affected by change in the peroxide concentration.

3.6. Choice of excitation wavelength

Different papers define various wavelengths for the excitation wavelengths. It was decided to verify the data and therefore an excitation scan was carried out for a 20 μM $\text{VO}(\text{acac})_2$. The emission wavelength was maintained at 429 nm and the excitation spectrum was measured. The highest intensity for excitation was observed at ~ 312 nm.

4. CONCLUSIONS

4.1. Aqueous system

The system was first tested in the aqueous system. When concentrated peroxide (~9M) was used, the maximum fluorescence intensity of 2-OH-TPA formed decreased over time. This was related to polyhydroxylation of the TPA molecule. However, when a peroxide concentration of ~1,8 mM was used, the signal of the formed 2-OH-TPA in the sample increased over time. An increase in fluorescence with an increase in vanadium complex concentration was observed. A good sensitivity was obtained with 1,8 mM H₂O₂. The LOD for vanadium was determined to be 4 μM.

4.2. Aqueous system containing galactose

The system was then tested in aqueous system with galactose to provide a matrix as similar as possible to the agarose gel. The system has a good working range for upto 300 μM when of 0,50% galactose was present. The sensitivity decreased significantly during the presence of galactose. The LOD for vanadium was established to be 5 μM.

4.3. Agarose gels

The system was finally tested in agarose gels. The sensitivity in agarose gels is worse than the system containing agarose gels. There were major issues in homogeneity during preparation of the gel. In gels where homogeneity was achieved, a small hump was observed in the region where 2-OH-TPA emits. A different sample preparation technique should be used in the future. The concentrated vanadium complexes/H₂O₂ could be added in the gel containing TPA while the gel is solidifying.

4.4. Overall

Due to time restrictions it was not possible to complete the development of this method. Even though the studies in the agarose matrix were not complete, the method has shown promising results in aqueous solutions. The interference from high concentrations of galactose decreased sensitivity, but did not affect the limit of detection significantly. The future optimization of the gel conditions when using agarose matrices should also give good results. This will provide a new method that can be used to complement existing ones in the study of metal binding to DNA, and provide useful insights into the nature of metal-DNA interactions.

5. BIBLIOGRAPHY

5.1. References

-
- ¹ Radzicka A., Wolfenden R., *Science*, **1995**, 267, 5194, 90-93.
- ² Williams N. H., Takasaki B., Wall B., Chin J., *Accounts of Chemical Research*, **1999**, 32, 485-493
- ³ Mancin F., Teclilla P. in *Metal Complex-DNA Interactions*, Hadjiliadis N., Sletten E., Blackwell Publishing Ltd.
- ⁴ Cowan J. A., *Chemical Reviews*, **1998**, 98, 1067-1087.
- ⁵ Sträter N., Lipscomb W. N., Klabunde T., Krebs B., *Angewandte Chemie International Edition in English*, **1996**, 35, 18, 2024-2055.
- ⁶ Sinden R. R., Pearson C. E., Potaman V. N., Ussery D. W., *Advances in Genome Biology*, **1998**, 5A, 1-141, JAI Press Inc.
- ⁷ Pessoa J. C., Tomaz I., *Current medicinal Chemistry*, **2010**, 17, 3701-3738.
- ⁸ Butenko N., Tomaz A. I., Nouri O., Escribano E., Moreno V., Gama S., Ribeiro V., Telo J. P., Pessoa J. C., Cavaco I., *Journal of Inorganic Biochemistry*, **2009**, 103, 622-632.
- ⁹ Baslie L., Barton J.K., *Journal of American Chemical Society*, **1987**, 109, 24, 7548-7550.
- ¹⁰ Takeda N., Shibata M., Tajima N., Hirao K., Komiyama M., *Journal of Organic Chemistry*, **2000**, 65, 4391-4396.
- ¹¹ Fife T. H., Przystas T. J., *Journal of American Chemical Society*, **1982**, 104, 2251-2257.
- ¹² Jiang Q., Xiao N., Shi P., Zhu Y., Guo Z., *Coordination Chemistry Reviews* **2007**, 251, 1951-1972.
- ¹³ Kuzntsova A. A., Knorre D. G., Deorova O. S., *Russian Chemical Reviews* **2009**, 78, 7, 659-678.
- ¹⁴ Pogozelski W. K., Tullius T. D., *Chemical Reviews*, **1998**, 98, 1089-1107.
- ¹⁵ Burger R. M., *Chemical Reviews*, **1998**, 98, 1153-1169.

-
- ¹⁶ Rosenberg B., Vancamp L., Trosko J. E., Mansour V. H., *Nature*, **1969**, 222, 385-386.
- ¹⁷ Nunez M. E., Barton J.K., *Current opinion in Chemical Biology*, **2000**, 4, 2, 199-206.
- ¹⁸ Wolkenberg S. E., Boger D. L., *Chemical Reviews*, **2002**, 102, 7, 2477-2495.
- ¹⁹ Tuillius T. D., Greenbaum J. A., *Current Opinion in Chemical Biology*, **2005**, 9, 2, 127-134.
- ²⁰ Mancin F., Scrimin P., Tecilla P., Tonellato U., *Chemical Communications*, **2005**, 2540-2548.
- ²¹ Tracey A. S., Willsky G. R., Tekeuchi E. S., *VANADIUM: Chemistry, Biochemistry, Pharmacology and Practical Applications*, **2007**, CRC Press.
- ²² Harris W. R., Friedman S. B., Silberman D., *Journal of Inorganic Chemistry*, **1984**, 157-169.
- ²³ Kiss T., Jakusch T., Hollander D., Dornyei A., Enyedy E. A., Pessoa J. C., Sakurai H., Sanz-Medel A., *Biospeciation of antidiabetic VO(IV) complexes*, *Coordination Chemistry Reviews*, **2008**, 252, 1153-1162.
- ²⁴ Crans D. C., *Journal of Inorganic Biochemistry*, **2000**, 80, 123-131.
- ²⁵ Shi X., Jiang H., Ye J., Saffiotti U., *Toxicology*, **1996**, 106, 27-38.
- ²⁶ Thompson K. H., Orvig C., *Journal of Inorganic Biochemistry*, **2006**, 1925-1935.
- ²⁷ Verquin G., Fontaine G., Bria M., Zhilinskaya E., Abi-Aad E., Aboukaïs A., Baldeyrou B., Bailly C., Bernier J., *Journal of Biological Inorganic Chemistry*, **2004**, 9, 345-353.
- ²⁸ Prasad P., Sasmal P. K., Majumdar R., Dighe R. R., Chakravarty A. R., *Inorganica Chimica Acta*, **2010**, 363, 2743-2751
- ²⁹ Sam M., Hwang J., Chanfreau G., Abu-Omar M. M., *Inorganic Chemistry*, **2004**, 43, 26, 8447-8455.
- ³⁰ Heater S. J., Carrano M. W., Rains D., Walter R. B., Ji D., Yan Q., Czernuszewicz R. S., Carrano C. J., *Inorganic Chemistry*, **2000**, 39, 3881-3889.
- ³¹ Alessio E., Mestroni G., Bergamo A., Sava G., *Current Topics in Medicinal Chemistry*, **2004**, 4, 1525-1535.
- ³² Dyson P. J., Sava G., *Dalton Transactions*, **2006**, 1929-1933.
- ³³ Hartinger C. G., Jakupec M. A., Zorbas-Seifried S., Groessler M., Egger A., Berger W., Zaboras H., Dyson P., Keppler B. K., *Chemistry and Biodiversity*, **2008**, 5, 2140-2155.
-

-
- ³⁴ Malina J., Novakova O., Keppler B. K., Alessio E., Brabec V., *Journal of Inorganic Biochemistry*, **2001**, 6, 435-445.
- ³⁵ Yan Y. K., Melchart M., Habtemariam A., Salder P. J., *Chemical Communicaitons*, **2005**, 2764-4776.
- ³⁶ Tan C., Liu J., Chen L., Shi S., Ji L., *Journal of Inorganic Biochemistry*, **2008**, 1644-1653.
- ³⁷ Deshpande M. S., Kumbhar A. A., Khumbar A. S., *Inorganic Chemistry*, **2007**, 46, 5450-5452.
- ³⁸ Janaratne T. K., Yadav. A., Onger F., MacDonnell M., *Inorganic Chemistry*, **2007**, 46, 3420-2422
- ³⁹ Otero L., Smircich P., Vieites M., Ciganda M., Severino P. C., Terenzi H., Cerecetto H., Gambino D., Garat B., *Journal of Inorganic Chemistry*, **2007**, 101, 74-79.
- ⁴⁰ Araki C., *Bulletin of the Chemical Society of Japan*, **1956**, 29, 4, 543-544.
- ⁴¹ Watson J. D., Baker T. A., Bell S. P., Gann A., Levine M., Losick, *Molecular Biology of the Gene*, **2004**, Pearson Education Publishers, California, USA.
- ⁴² Fenton H.J.H, *Journal of Chemical Society Transactions*, **1894**, 65, 899-911.
- ⁴³ Haber F., Weiss J., *Proceedings of Royal Society of London*, **1934**, 147, 332
- ⁴⁴ Barb W. G., Baxendale J. H., George P., Hargrave K. R., *Trans Faraday Society*, **1952**, 50, 375.
- ⁴⁵ Prousek J., *Chemicke Listy*, **1995**, 89, 11-21.
- ⁴⁶ Masarwa M., Cohen H., Meyerstein D., Hickman D. L., Bakac A., Espenson J. H., *Journal of American Chemical Society*, **1988**, 110, 4293-4297.
- ⁴⁷ Czapski G., Samuni A., Meisel D., *The Journal of Physical Chmistry*, **1971**, 75, 21, 3271-3280.
- ⁴⁸ Mussali-Galante P., Rodriguez-Lara V., Avila-Costa M. R., in *Vanadium: Its Impact on Health*, **2007**, Fortoul T. I., Avila-Costa M. R., Nova Science Publishers, USA.
- ⁴⁹ Barreto J. C., Smith G. S., Strobel N. H. P., McQuillin P. A., Miller T. A., *Pharmacology Letters*, **1995**, 56, 89-96.
- ⁵⁰ Armstrong W. A., Facey R. A., Grant D. W., Humphreys W. G., *Canadian Journal of Chemistry*, **1963**, 41.
- ⁵¹ Mason T. J., Lorimer J. P., Bates D. M., Zhao Y., *Ultrasonics Sonochemistry*, **1994**, 1, 2.

-
- ⁵² Mark G., Tauber A., Laupert R., Schuchmann H-P., Schulz D., Mues A., Sonntag C., *Ultrasonics Sonochemistry*, **1998**, 5, 41-52.
- ⁵³ Linxiang L., Abe Y., Nagasawa Y., Kudo R., Usui N., Imai K., Mashino T., Mochizuki M., Miyata N., *Biomedical Chromatography*, **2004**, 18, 470
- ⁵⁴ Bonner P. L. R., Hargreaves, *Bioscience Laboratory Techniques*, **2011**, Wiley-Blackwell Publishers, UK
- ⁵⁵ Martin R., *Gel Electrophoresis: Nucleic Acids*, **1996**, Bios Scientific Publishers, Oxford, UK.
- ⁵⁶ Pavia, Lampman, Kriz, Vyvyan, *Introduction to Spectroscopy*,**2009**, Fourth edition, Brooks/Cole, Cengage Learning Publishers, USA.
- ⁵⁷ Haven C. M., Tetrault G. A., Schenken J. R., *Laboratory Instrumentation*, **1995** Fourth edition, John Wiley and Sons Inc, USA.
- ⁵⁸ Ramsden E. N., *A-level Chemistry: Detection and Analysis*, **1996**, Stanley Thornes Publications, UK.
- ⁵⁹ Albani J. R., *Principles and Applications of Fluorescence Spectroscopy*, **2007**, Blackwell Publishing.
- ⁶⁰ Lakowicz J. R., *Principles of fluorescence spectroscopy*, **2006**, Third edition, Springer Publications.
- ⁶¹ Mueller S., Riedel H.D., Stremmel W., *Analytical Biochemistry* **1997**, 245, 55-60.